Nonlinear Pose Filters on the Special Euclidean Group SE(3) With Guaranteed Transient and Steady-State Performance

Hashim A. Hashim, *Student Member, IEEE*, Lyndon J. Brown, and Kenneth McIsaac, *Member, IEEE*

***Abstract*—Two novel nonlinear pose (i.e., attitude and position) filters developed directly on the Special Euclidean Group $\mathbb{SE}(3)$ able to guarantee prescribed characteristics of transient and steady-state performance are proposed. The position error and normalized Euclidean distance of attitude error are trapped to arbitrarily start within a given large set and converge systematically and asymptotically to the origin from almost any initial condition. The transient error is guaranteed not to exceed a prescribed value while the steady-state error is bounded by a predefined small value. The first pose filter operates based on a set of vectorial measurements coupled with a group of velocity vectors and requires preliminary pose reconstruction. The second filter, on the contrary, is able to perform its function using a set of vectorial measurements and a group of velocity vectors directly. Both proposed filters provide reasonable pose estimates with superior convergence properties while being able to use measurements obtained from low-cost inertial measurement, landmark measurement, and velocity measurement units. The simulation results demonstrate the effectiveness and robustness of the proposed filters considering large error in initialization and high level of uncertainties in velocity vectors as well as in the set of vector measurements.**

***Index Terms*—Attitude, feature measurement, inertial measurement unit (IMU), nonlinear observer, pose estimation, position, prescribed performance function (PPF), $\mathbb{SE}(3)$, $\mathbb{SO}(3)$, Special Euclidean Group, Special Orthogonal Group, steady-state error, transformed error, transient.**

I. Introduction

ROBOTICS and engineering applications, such as aerial and underwater vehicles, satellites, and space crafts, are concerned with accurately estimating the pose of a rigid-body in three-dimensional (3-D) space. In essence, the pose of a rigid-body consists of two elements: 1) orientation and 2) position. The orientation of a rigid-body in 3-D space is often referred to as attitude, therefore, orientation and attitude will be used interchangeably. One of the basic methods of attitude reconstruction is the algebraic approach. It allows to reconstruct the attitude given by the availability of two or more noncollinear inertial-frame vectors and their body-frame vectors utilizing algorithms, such as QUEST [1] or singular value decomposition (SVD) [2]. However, the process of attitude reconstruction is vulnerable to the effects of noise and bias contaminating the body-frame measurements which causes [1], [2] to produce unsatisfactory results. This is particularly true in the context of a rigid-body fitted with low-cost inertial measurement unit (IMU) [3].

Gaussian filters or nonlinear deterministic filters have been used historically to address the challenge of attitude estimation [3]. The family of Gaussian filters, which includes Kalman filter (KF) [4], extended KF (EKF) [5], and multiplicative EKF (MEKF) [6], often consider the unit quaternion in attitude representation [3]. For good survey of Gaussian filters please see [3]. However, it is crucial to note the nonlinear nature of the attitude problem [3]. Nonlinear attitude filters such as [3] and [7]–[10] are evolved directly on the Special Orthogonal Group $\mathbb{SO}(3)$. In particular, nonlinear deterministic attitude filters outperform the Gaussian filters in many respects, namely they are simpler in derivation and representation, they demand less processing power, and they show better tracking convergence [3], [7]. Attitude estimation is an essential part of the pose estimation problem. Taking into consideration the remarkable advantages of nonlinear attitude filters, attitude-position (pose) filtering problem is the best approached in a nonlinear sense.

The pose estimation problem relies on filters evolved on the Special Euclidean Group $\mathbb{SE}(3)$ which require a measurement derived from a group velocity vector, vectorial measurements that could be provided by IMU, landmark measurements collected, for example, by a vision system and an estimate of the bias associated with velocity measurements. Pose estimation commonly involves a computer vision system with a monocular camera and IMU [11]–[13]. The pose filter described in [12] was developed directly on $\mathbb{SE}(3)$ and its performance has been proven to be exponentially stable. Although, the filter in [12] requires pose reconstruction for the implementation, the nonlinear filter can be modified to function-based solely on a set of vectorial measurements avoiding the need for pose reconstruction [14], [15]. In spite of the simplicity of the filter design in [12], [14], and [15], numerical results show high sensitivity to noise and bias attached to the measurements. In addition, no systematic convergence is observed in [11]–[18], such that the tracking error does not follow a

Manuscript received February 25, 2019; accepted May 25, 2019. This work was supported in part by the Natural Sciences and Engineering Research Council of Canada (NSERC) Discovery Grant Program. This paper was recommended by Associate Editor Q. Ge. *(Corresponding author: Hashim A. Hashim.)*

The authors are with the Department of Electrical and Computer Engineering, University of Western Ontario, London, ON N6A 5B9, Canada (e-mail: hmoham33@uwo.ca; lbrown@uwo.ca; kmcisaac@uwo.ca).

Color versions of one or more of the figures in this paper are available online at http://ieeexplore.ieee.org.

Digital Object Identifier 10.1109/TSMC.2019.2920114

predefined transient and steady-state measures. Accordingly, successful pose estimation for spacecraft control applications, such as [19]–[22], cannot be achieved without pose filters which are robust against uncertain measurements, demonstrate the fast tracking performance, and satisfy a certain level of transient and steady-state characteristics.

Prescribed performance implies confining the error to initially start within a predefined large set and decay systematically and smoothly to a predefined small residual set [23]. The error trajectory is constrained by a prescribed performance function (PPF) to satisfy transient as well as steady-state performance. The main objective of prescribed performance is to relax the constrained error to its unconstrained form, termed transformed error, which allows to keep the error within the decaying dynamic boundaries, and thereby achieve successful estimation or control applications. These applications include, but are not limited to, two degrees of freedom planar robots [23], [24], uncertain nonlinear systems [25], servo mechanism with friction compensation [26], and uncertain multiagent system [27], [28].

In this paper, two robust nonlinear pose filters on $\mathbb{SE}(3)$ with predefined transient as well as steady-state measures are proposed. The main contributions are as follows.

1) The proposed filters guarantee boundedness of the closed-loop error signals with constrained error and unconstrained transformed error being proven to be almost globally asymptotically stable such that the error in the homogeneous transformation matrix is regulated asymptotically to the identity from almost any initial condition. Most significantly, the exceptional performance is guaranteed even when the measurements are supplied by a low-cost measurement unit, for instance, an IMU module equipped with a gyroscope, a vision unit, and a GPS.
2) The proposed filters guarantee systematic convergence of the error controlled by the dynamic reducing boundaries forcing the error to start within a predefined large set and decrease systematically and smoothly to a residual small set, unlike [11]–[16].
3) The proposed pose filters are more efficient at ensuring fast convergence compared to similar estimators described in the literature, for instance [11]–[16].

The fast convergence is mainly attributed to the dynamic behavior of the estimator gains. The first filter requires a group of velocity vectors and a set of measurements to obtain an online algebraic reconstruction of the pose. The second filter uses the group of velocity vector and the set of vectorial measurements directly.

The remainder of this paper is organized as follows. Section II gives an overview of $\mathbb{SO}(3)$ and $\mathbb{SE}(3)$, and mathematical notation and identities. The pose problem is formulated, vector measurements are demonstrated and prescribed performance is introduced in Section III. The two proposed filters and the related stability analysis are presented in Section IV. Section V elaborates on the effectiveness and robustness of the proposed filters. Finally, Section VI draws a conclusion of this paper.

II. Preliminaries and Mathematical Identities

In this paper, $\mathbb{R}_+$ refers to the set of non-negative real numbers. $\mathbb{R}^n$ and $\mathbb{R}^{n\times m}$ denote a real n-dimensional space column vector and real $n \times m$ dimensional space, respectively. The Euclidean norm of $x \in \mathbb{R}^n$ is $\|x\| = \sqrt{x^\top x}$ with $^\top$ being the transpose of the component. $\lambda(\cdot)$ denotes a set of singular values of a matrix with $\underline{\lambda}(\cdot)$ being its minimum value. $\mathbf{I}_n$ stands for an n-by-n identity matrix, while $\underline{\mathbf{0}}_n \in \mathbb{R}^n$ is a zero column vector. The frame notation is as follows: $\{\mathcal{B}\}$ refers to the body-frame and $\{\mathcal{I}\}$ represents the inertial-frame.

Define $\mathbb{GL}(3)$ as a 3-D general linear group which is a Lie group with smooth multiplication and inversion. The orthogonal group, denoted by $\mathbb{O}(3)$, is a subgroup of $\mathbb{GL}(3)$ defined by

$$\mathbb{O}(3) = \left\{ M \in \mathbb{R}^{3\times 3} \middle| M^\top M = MM^\top = \mathbf{I}_3 \right\}$$

with $\mathbf{I}_3$ being a 3-by-3 identity matrix. Let $\mathbb{SO}(3)$ denote the Special Orthogonal Group which is a subgroup of $\mathbb{O}(3)$. The orientation of a rigid-body in 3-D space is termed attitude, denoted by R, and defined as follows:

$$\mathbb{SO}(3) = \left\{ R \in \mathbb{R}^{3\times 3} \middle| RR^\top = R^\top R = \mathbf{I}_3, \det(R) = +1 \right\}$$

with $\det(\cdot)$ being the determinant of the associated matrix. $\mathbb{SE}(3)$ stands for the Special Euclidean Group, a subset of the affine group $\mathbb{GA}(3) = \mathbb{SO}(3) \times \mathbb{R}^3$ defined by

$$\mathbb{SE}(3) = \left\{ \boldsymbol{T} \in \mathbb{R}^{4\times 4} \middle| R \in \mathbb{SO}(3), P \in \mathbb{R}^3 \right\}$$

where $\boldsymbol{T} \in \mathbb{SE}(3)$, termed a homogeneous transformation matrix, represents the pose of a rigid-body in 3-D space with

$$\boldsymbol{T} = \begin{bmatrix} R & P \\ \underline{\mathbf{0}}_3^\top & 1 \end{bmatrix} \in \mathbb{SE}(3) \tag{1}$$

where $P \in \mathbb{R}^3$ and $R \in \mathbb{SO}(3)$ denote the position and attitude of a rigid-body in 3-D space, respectively, and $\underline{\mathbf{0}}_3^\top$ is a zero row. $\mathfrak{so}(3)$ is a Lie algebra related to $\mathbb{SO}(3)$ defined by

$$\mathfrak{so}(3) = \left\{ A \in \mathbb{R}^{3\times 3} \middle| A^\top = -A \right\}$$

where A is a skew symmetric matrix. Define the map $[\cdot]_\times : \mathbb{R}^3 \to \mathfrak{so}(3)$ as

$$[\alpha]_\times = \begin{bmatrix} 0 & -\alpha_3 & \alpha_2 \\ \alpha_3 & 0 & -\alpha_1 \\ -\alpha_2 & \alpha_1 & 0 \end{bmatrix} \in \mathfrak{so}(3), \alpha = \begin{bmatrix} \alpha_1 \\ \alpha_2 \\ \alpha_3 \end{bmatrix}.$$

For any $\alpha, \beta \in \mathbb{R}^3$, we define $[\alpha]_\times \beta = \alpha \times \beta$ with $\times$ being the cross product. The wedge operator is denoted by $\wedge$, and for any $\mathcal{Y} = [y_1^\top, y_2^\top]^\top$ with $y_1, y_2 \in \mathbb{R}^3$ the wedge map $[\cdot]_\wedge : \mathbb{R}^6 \to \mathfrak{se}(3)$ is defined by

$$[\mathcal{Y}]_\wedge = \begin{bmatrix} [y_1]_\times & y_2 \\ \underline{\mathbf{0}}_3^\top & 0 \end{bmatrix} \in \mathfrak{se}(3)$$

$\mathfrak{se}(3)$ is a Lie algebra of $\mathbb{SE}(3)$ and can be expressed as

$$\mathfrak{se}(3) = \left\{ [\mathcal{Y}]_\wedge \in \mathbb{R}^{4\times 4} \middle| \exists y_1, y_2 \in \mathbb{R}^3 : [\mathcal{Y}]_\wedge = \begin{bmatrix} [y_1]_\times & y_2 \\ \underline{\mathbf{0}}_3^\top & 0 \end{bmatrix} \right\}.$$

The inverse of $[\cdot]_\times$ is defined by $\mathbf{vex} : \mathfrak{so}(3) \to \mathbb{R}^3$, and for $\alpha \in \mathbb{R}^3$ and $[\alpha]_\times \in \mathfrak{so}(3)$, we have

$$\mathbf{vex}\big([\alpha]_\times\big) = \alpha \in \mathbb{R}^3. \tag{2}$$

$\mathcal{P}_a$ stands for an anti-symmetric projection operator on the Lie algebra $\mathfrak{so}(3)$ while its mapping is given by $\mathcal{P}_a : \mathbb{R}^{3\times3} \to \mathfrak{so}(3)$ such that

$$\mathcal{P}_a(M) = \frac{1}{2}\Big(M - M^\top\Big) \in \mathfrak{so}(3),\ M \in \mathbb{R}^{3\times3}. \tag{3}$$

The normalized Euclidean distance of the attitude matrix $R \in \mathbb{SO}(3)$ is given by

$$\|R\|_I = \frac{1}{4}\mathrm{Tr}\{\mathbf{I}_3 - R\} \tag{4}$$

with $\mathrm{Tr}\{\cdot\}$ being a trace of a matrix, while $\|R\|_I \in [0, 1]$. To reconstruct the orientation of any rigid-body in 3-D space, it is sufficient to know unit-axis $u \in \mathbb{R}^3$ in the sphere $\mathbb{S}^2$ and angle of rotation $\alpha \in \mathbb{R}$ about u. This type of parameterization is termed angle-axis parameterization and its mapping to $\mathbb{SO}(3)$ is given by $\mathcal{R}_\alpha : \mathbb{R} \times \mathbb{R}^3 \to \mathbb{SO}(3)$ such that

$$\mathcal{R}_\alpha(\alpha, u) = \mathbf{I}_3 + \sin(\alpha)[u]_\times + (1 - \cos(\alpha))[u]_\times^2. \tag{5}$$

For $\alpha, \beta \in \mathbb{R}^3$, $R \in \mathbb{SO}(3)$, $A \in \mathbb{R}^{3\times3}$, and $B = B^\top \in \mathbb{R}^{3\times3}$, the following mathematical identities:

$$[\alpha \times \beta]_\times = \beta\alpha^\top - \alpha\beta^\top \tag{6}$$

$$[R\alpha]_\times = R[\alpha]_\times R^\top \tag{7}$$

$$[\alpha]_\times^2 = -\alpha^\top\alpha\mathbf{I}_3 + \alpha\alpha^\top \tag{8}$$

$$B[\alpha]_\times + [\alpha]_\times B = \mathrm{Tr}\{B\}[\alpha]_\times - [B\alpha]_\times \tag{9}$$

$$\mathrm{Tr}\big\{B[\alpha]_\times\big\} = 0 \tag{10}$$

$$\mathrm{Tr}\big\{A[\alpha]_\times\big\} = \mathrm{Tr}\big\{\mathcal{P}_a(A)[\alpha]_\times\big\} = -2\mathbf{vex}(\mathcal{P}_a(A))^\top\alpha \tag{11}$$

will be used in the subsequent derivations.

III. Problem Formulation With Prescribed Performance

Pose estimator relies on a set of vectorial measurements made on inertial-frame and body-frame. This section aims to define the pose problem and present the associated measurements. Next, the pose error and its reformulation are geared toward attaining desired characteristics of the transient and steady-state performance.

A. Pose Kinematics and Measurements

The pose of any rigid-body in 3-D space consists of two elements: attitude and position, and this paper aims to estimate both elements. The attitude of a rigid-body is commonly represented by a rotational matrix $R \in \mathbb{SO}(3)$ defined relative to the body-frame such that $R \in \{\mathcal{B}\}$. Position of a rigid-body is, on the contrary, defined by $P \in \mathbb{R}^3$ with respect to the inertial-frame $P \in \{\mathcal{I}\}$. The pose problem can be characterized by the homogeneous transformation matrix $\boldsymbol{T} \in \mathbb{SE}(3)$ as

$$\boldsymbol{T} = \begin{bmatrix} R & P \\ \mathbf{0}_3^\top & 1 \end{bmatrix}. \tag{12}$$

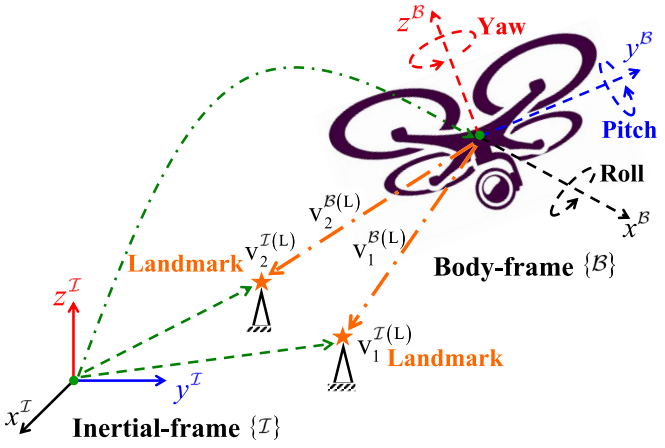

Fig. 1. Pose estimation problem of a rigid-body in 3-D space.

The pose estimation problem of a rigid-body in 3-D space is depicted in Fig. 1.

Let the components associated with body-frame and inertial-frame be assigned superscripts $\mathcal{B}$ and $\mathcal{I}$, respectively. The attitude can be obtained given N_R known noncollinear inertial vectors, available for measurements at a coordinate fixed to the moving body. IMU exemplify sensors, which could provide those measurements. The ith body-frame vector measurement is given by

$$\begin{bmatrix} v_i^{\mathcal{B}(R)} \\ 0 \end{bmatrix} = \boldsymbol{T}^{-1}\begin{bmatrix} v_i^{\mathcal{I}(R)} \\ 0 \end{bmatrix} + \begin{bmatrix} b_i^{\mathcal{B}(R)} \\ 0 \end{bmatrix} + \begin{bmatrix} \omega_i^{\mathcal{B}(R)} \\ 0 \end{bmatrix}$$

such that

$$v_i^{\mathcal{B}(R)} = R^\top v_i^{\mathcal{I}(R)} + b_i^{\mathcal{B}(R)} + \omega_i^{\mathcal{B}(R)} \tag{13}$$

with $v_i^{\mathcal{I}(R)}$ being the ith known vector in the inertial-frame, and $b_i^{\mathcal{B}(R)}$ and $\omega_i^{\mathcal{B}(R)}$ being the unknown bias and noise components added to the ith measurement, respectively, for all $v_i^{\mathcal{B}(R)}, v_i^{\mathcal{I}(R)}, b_i^{\mathcal{B}(R)}, \omega_i^{\mathcal{B}(R)} \in \mathbb{R}^3$ and $i = 1, 2, \ldots, N_R$. The known inertial vector $v_i^{\mathcal{I}(R)}$ and the available body-frame measurement $v_i^{\mathcal{B}(R)}$ in (13) can be normalized such that

$$\upsilon_i^{\mathcal{I}(R)} = \frac{v_i^{\mathcal{I}(R)}}{\big\|v_i^{\mathcal{I}(R)}\big\|}$$
$$\upsilon_i^{\mathcal{B}(R)} = \frac{v_i^{\mathcal{B}(R)}}{\big\|v_i^{\mathcal{B}(R)}\big\|}. \tag{14}$$

Thus, the attitude of a rigid-body can be extracted using $\upsilon_i^{\mathcal{I}(R)}$ and $\upsilon_i^{\mathcal{B}(R)}$ in (14) rather than $v_i^{\mathcal{I}(R)}$ and $v_i^{\mathcal{B}(R)}$. Let us introduce the following two sets:

$$\upsilon^{\mathcal{I}(R)} = \Big[\upsilon_1^{\mathcal{I}(R)}, \ldots, \upsilon_{N_R}^{\mathcal{I}(R)}\Big] \in \{\mathcal{I}\}$$
$$\upsilon^{\mathcal{B}(R)} = \Big[\upsilon_1^{\mathcal{B}(R)}, \ldots, \upsilon_{N_R}^{\mathcal{B}(R)}\Big] \in \{\mathcal{B}\} \tag{15}$$

where the two sets in (15) include the normalized vectors in (14) for all $\upsilon^{\mathcal{I}(R)}, \upsilon^{\mathcal{B}(R)} \in \mathbb{R}^{3\times N_R}$. The position of the moving body can be extracted if its attitude R has already

been determined and there exist N_L known landmarks (feature points) obtained, for example, by a vision system. The ith body-frame landmark measurement is given by

$$\begin{bmatrix} v_i^{\mathcal{B}(L)} \\ 1 \end{bmatrix} = \boldsymbol{T}^{-1} \begin{bmatrix} v_i^{\mathcal{I}(L)} \\ 1 \end{bmatrix} + \begin{bmatrix} b_i^{\mathcal{B}(L)} \\ 0 \end{bmatrix} + \begin{bmatrix} \omega_i^{\mathcal{B}(L)} \\ 0 \end{bmatrix}$$

such that

$$v_i^{\mathcal{B}(L)} = R^\top \Big(v_i^{\mathcal{I}(L)} - P \Big) + b_i^{\mathcal{B}(L)} + \omega_i^{\mathcal{B}(L)} \tag{16}$$

where $v_i^{\mathcal{I}(L)}$ is the ith known fixed landmark located in the inertial-frame, $b_i^{\mathcal{B}(L)}$ and $\omega_i^{\mathcal{B}(L)}$ are the additive unknown bias and noise vectors of the ith measurement, respectively, for all $v_i^{\mathcal{B}(L)}, v_i^{\mathcal{I}(L)}, b_i^{\mathcal{B}(L)}, \omega_i^{\mathcal{B}(L)} \in \mathbb{R}^3$ and $i = 1, 2, \ldots, N_L$. Define the set of inertial-frame and body-frame vectors associated with landmarks by

$$\begin{aligned} v^{\mathcal{B}(L)} &= \left[v_1^{\mathcal{B}(L)}, \ldots, v_{N_L}^{\mathcal{B}(L)} \right] \in \{\mathcal{B}\} \\ v^{\mathcal{I}(L)} &= \left[v_1^{\mathcal{I}(L)}, \ldots, v_{N_L}^{\mathcal{I}(L)} \right] \in \{\mathcal{I}\}. \end{aligned} \tag{17}$$

In case when more than one landmark is available for measurement, it is common to obtain a weighted geometric center of all the landmarks, which can be calculated as follows:

$$\mathcal{G}_c^{\mathcal{I}} = \frac{1}{\sum_{i=1}^{N_L} k_i^L} \sum_{i=1}^{N_L} k_i^L v_i^{\mathcal{I}(L)} \tag{18}$$

$$\mathcal{G}_c^{\mathcal{B}} = \frac{1}{\sum_{i=1}^{N_L} k_i^L} \sum_{i=1}^{N_L} k_i^L v_i^{\mathcal{B}(L)} \tag{19}$$

such that k_i^L is the confidence level of the ith measurement.

Assumption 1 (Rigid-Body Pose Observability): The pose of a rigid-body in 3-D space can be extracted given the availability of at least two noncollinear vectors from the sets in (15) ($N_R \geq 2$) and at least one feature point from the sets in (17) with $N_L \geq 1$. In the case when $N_R = 2$, the third vector can be obtained by the means of cross multiplication: $\upsilon_3^{\mathcal{I}(R)} = \upsilon_1^{\mathcal{I}(R)} \times \upsilon_2^{\mathcal{I}(R)}$ and $\upsilon_3^{\mathcal{B}(R)} = \upsilon_1^{\mathcal{B}(R)} \times \upsilon_2^{\mathcal{B}(R)}$.

According to Assumption 1, a set of vectorial measurement described in (15) is sufficient to have rank 3 provided that $N_R \geq 2$. Accordingly, the homogeneous transformation matrix $\boldsymbol{T}$ can be extracted if Assumption 1 is met. For simplicity, the body-frame vectors $v_i^{\mathcal{B}(R)}$ and $v_i^{\mathcal{B}(L)}$ are considered to be noise and bias free in the stability analysis. In Section V, on the contrary, the noise and bias corrupting the measurements of $v_i^{\mathcal{B}(R)}$ and $v_i^{\mathcal{B}(L)}$ are taken into consideration. The pose kinematics of the homogeneous transformation matrix $\boldsymbol{T}$ in (12) are given by

$$\begin{bmatrix} \dot{R} & \dot{P} \\ \underline{\mathbf{0}}_3^\top & 0 \end{bmatrix} = \begin{bmatrix} R & P \\ \underline{\mathbf{0}}_3^\top & 1 \end{bmatrix} \begin{bmatrix} [\Omega]_\times & V \\ \underline{\mathbf{0}}_3^\top & 0 \end{bmatrix}$$

such that

$$\dot{P} = RV$$

$$\dot{R} = R[\Omega]_\times \tag{20}$$

$$\dot{\boldsymbol{T}} = \boldsymbol{T}[\mathcal{Y}]_\wedge \tag{21}$$

with $\Omega \in \mathbb{R}^3$ and $V \in \mathbb{R}^3$ being the true angular and translational velocity of the moving body, respectively, and $\mathcal{Y} = [\Omega^\top, V^\top]^\top \in \mathbb{R}^6$ being the group velocity vector. The angular velocity can be measured by a gyroscope, for example, and expressed as follows:

$$\Omega_m = \Omega + b_\Omega + \omega_\Omega \in \{\mathcal{B}\} \tag{22}$$

where b_Ω is an unknown constant or slowly time-varying bias, and ω_Ω is an unknown random noise attached to the measurement, for all $b_\Omega, \omega_\Omega \in \mathbb{R}^3$. Likewise, the translational velocity measurement of a moving body can be obtained using a GPS, for instance, and defined by

$$V_m = V + b_V + \omega_V \in \{\mathcal{B}\} \tag{23}$$

with $b_V \in \mathbb{R}^3$ denoting an unknown constant or slowly time-varying bias, and $\omega_V \in \mathbb{R}^3$ being random noise attached to the translational velocity measurements. The group of velocity measurements and bias associated with it can be defined by $\mathcal{Y}_m = [\Omega_m^\top, V_m^\top]^\top \in \mathbb{R}^6$ and $b = [b_\Omega^\top, b_V^\top]^\top \in \mathbb{R}^6$, respectively. For the sake of simplicity, we consider $\omega_\Omega = \omega_V = \underline{\mathbf{0}}_3$ in the analysis. However, in the implementation, it is used $\omega_\Omega \neq \underline{\mathbf{0}}_3$ and $\omega_V \neq \underline{\mathbf{0}}_3$. Considering the normalized Euclidean distance of the rotational matrix R in (4) and the identity in (11), the true attitude kinematics in (20) can be expressed in view of (4) as

$$\begin{aligned} ||\dot{R}||_I &= -\frac{1}{4} \mathrm{Tr}\{\dot{R}\} \\ &= -\frac{1}{4} \mathrm{Tr}\{\boldsymbol{\mathcal{P}}_a(R)[\Omega]_\times\} \\ &= \frac{1}{2} \mathbf{vex}(\boldsymbol{\mathcal{P}}_a(R))^\top \Omega. \end{aligned} \tag{24}$$

Accordingly, the problem of pose kinematics in (21) can be reformulated and expressed in vector form as

$$\begin{bmatrix} ||\dot{R}||_I \\ \dot{P} \end{bmatrix} = \begin{bmatrix} \frac{1}{2} \mathbf{vex}(\boldsymbol{\mathcal{P}}_a(R))^\top & \underline{\mathbf{0}}_3^\top \\ \mathbf{0}_{3\times 3} & R \end{bmatrix} \begin{bmatrix} \Omega_m - b_\Omega \\ V_m - b_V \end{bmatrix} \tag{25}$$

with $\mathbf{0}_{3\times 3}$ being a zero matrix and $\omega_\Omega = \omega_V = \underline{\mathbf{0}}_3$. Let the estimate of the homogeneous transformation matrix in (12), denoted by $\hat{\boldsymbol{T}}$, be given by

$$\hat{\boldsymbol{T}} = \begin{bmatrix} \hat{R} & \hat{P} \\ \underline{\mathbf{0}}_3^\top & 1 \end{bmatrix} \tag{26}$$

with $\hat{R}$ and $\hat{P}$ being the estimates of R and P, respectively. Let us define the error in the homogeneous transformation matrix from body-frame to estimator-frame by

$$\tilde{\boldsymbol{T}} = \hat{\boldsymbol{T}} \boldsymbol{T}^{-1} = \begin{bmatrix} \tilde{R} & \hat{P} - \tilde{R}P \\ \underline{\mathbf{0}}_3^\top & 1 \end{bmatrix} = \begin{bmatrix} \tilde{R} & \tilde{P} \\ \underline{\mathbf{0}}_3^\top & 1 \end{bmatrix} \tag{27}$$

where $\tilde{R} = \hat{R}R^\top$ and $\tilde{P}$ are the errors associated with attitude and position, respectively. The aim of this paper is to drive $\hat{\boldsymbol{T}} \to \boldsymbol{T}$ which in turn guarantees driving $\tilde{P} \to \underline{\mathbf{0}}_3$, $\tilde{R} \to \mathbf{I}_3$, and $\tilde{\boldsymbol{T}} \to \mathbf{I}_4$. Lemma 1 will prove useful in the subsequent filter derivation.

Lemma 1: Let $R \in \mathbb{SO}(3)$, $M = M^\top \in \mathbb{R}^{3\times 3}$, M have rank 3, $\mathrm{Tr}\{M\} = 3$, and $\bar{\mathbf{M}} = \mathrm{Tr}\{M\}\mathbf{I}_3 - M$, while the minimum singular value of $\bar{\mathbf{M}}$ is $\underline{\lambda} \coloneqq \underline{\lambda}(\bar{\mathbf{M}})$. Then, the following holds:

$$||\mathbf{vex}(\boldsymbol{\mathcal{P}}_a(R))||^2 = 4(1 - ||R||_I)||R||_I \tag{28}$$

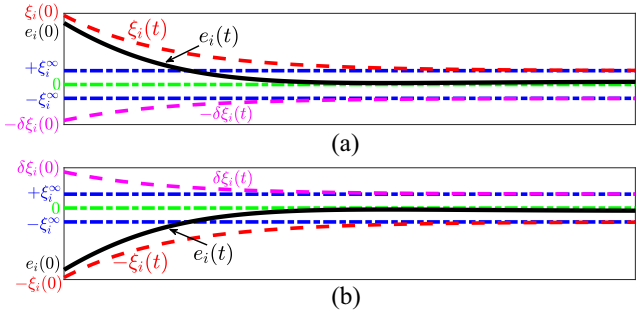

Fig. 2. Graphical representation of the systematic convergence of tracking error $\boldsymbol{e}_i$ with PPF satisfying (a) (32) and (b) (33).

$$\frac{2}{\underline{\lambda}}\frac{||\mathbf{vex}(\mathcal{P}_a(RM))||^2}{1+\mathrm{Tr}\{RMM^{-1}\}} \geq \|RM\|_I. \tag{29}$$

Proof: See the Appendix. ■

B. Prescribed Performance

Considering the error in the homogeneous transformation matrix as in (27) and in view of the pose kinematics in (25), let us define the error in vector form by

$$\boldsymbol{e} = [\boldsymbol{e}_1, \boldsymbol{e}_2, \boldsymbol{e}_3, \boldsymbol{e}_4]^\top = \left[||\tilde{R}||_I, \tilde{P}^\top\right]^\top \in \mathbb{R}^4. \tag{30}$$

The objective of this section is to reformulate the problem such that the error in (30) satisfies transient as well as steady-state measures predefined by the user. This can be achieved by guiding the error vector $\boldsymbol{e}$ to initiate within a large known set and after decaying smoothly and systematically settle within a predefined small set using PPF [23], [27]. The PPF is defined by $\xi_i(t)$ which is a positive smooth time-decreasing function which satisfies $\xi_i : \mathbb{R}_+ \to \mathbb{R}_+$ and $\lim_{t\to\infty}\xi_i(t) = \xi_i^\infty > 0$ and can be expressed by [23]

$$\xi_i(t) = \left(\xi_i^0 - \xi_i^\infty\right)\exp(-\ell_i t) + \xi_i^\infty \tag{31}$$

with $\xi_i(0) = \xi_i^0$ being the initial value of the PPF and the upper bound of the known large set, ξ_i^∞ being the upper bound of the narrow set, and ℓ_i being a positive constant controlling the convergence rate of $\xi(t)$ from ξ_i^0 to ξ_i^∞ for all $i = 1, \ldots, 4$. The error $\boldsymbol{e}_i(t)$ is guaranteed to follow the predefined transient and steady-state boundaries, if the conditions below are met:

$$-\delta\xi_i(t) < \boldsymbol{e}_i(t) < \xi_i(t), \quad \text{if } \boldsymbol{e}_i(0) > 0 \tag{32}$$

$$-\xi_i(t) < \boldsymbol{e}_i(t) < \delta\xi_i(t), \quad \text{if } \boldsymbol{e}_i(0) < 0 \tag{33}$$

with $\delta \in [0, 1]$. For clarity, define $\boldsymbol{e}_i \coloneqq \boldsymbol{e}_i(t)$ and $\xi_i \coloneqq \xi_i(t)$. Also, let us define $\xi = [\xi_1, \xi_2, \xi_3, \xi_4]^\top$, $\ell = [\ell_1, \ell_2, \ell_3, \ell_4]^\top$, $\xi^0 = [\xi_1^0, \xi_2^0, \xi_3^0, \xi_4^0]^\top$, and $\xi^\infty = [\xi_1^\infty, \xi_2^\infty, \xi_3^\infty, \xi_4^\infty]^\top$ for all $\xi, \ell, \xi^0, \xi^\infty \in \mathbb{R}^4$. The systematic convergence of the tracking error $\boldsymbol{e}_i$, from a given large set to a given narrow set in accordance with (32) and (33) is depicted in Fig. 2.

Remark 1: In accordance with the discussion in [23] and [27], knowing the upper bound and the sign of $\boldsymbol{e}_i(0)$ is sufficient to force the error to satisfy the performance constraints and maintain the error regulation within predefined dynamically reducing boundaries for all $t > 0$. If the condition in (32) or (33) is met, the maximum overshoot is sufficient to be bounded by $\pm\delta\xi_i$, the steady-state error is bounded by $\pm\xi_i^\infty$, and $|\boldsymbol{e}_i|$ is trapped between ξ_i and $\delta\xi_i$ as presented in Fig. 2.

Define the error $\boldsymbol{e}_i$ by

$$\boldsymbol{e}_i = \xi_i \mathcal{Z}(\mathcal{E}_i) \tag{34}$$

where $\xi_i \in \mathbb{R}$ is defined in (31), $\mathcal{E}_i \in \mathbb{R}$ is a relaxed form of the constrained error referred to as transformed error, and $\mathcal{Z}(\mathcal{E}_i)$ is a smooth function that behaves according to Assumption 2.

Assumption 2: The smooth function $\mathcal{Z}(\mathcal{E}_i)$ has the following properties [23].

1) $\mathcal{Z}(\mathcal{E}_i)$ is smooth and strictly increasing.
2) $\mathcal{Z}(\mathcal{E}_i)$ is constrained by the following two bounds:
   $-\underline{\delta}_i < \mathcal{Z}(\mathcal{E}_i) < \bar{\delta}_i$, if $\boldsymbol{e}_i(0) \geq 0$
   $-\bar{\delta}_i < \mathcal{Z}(\mathcal{E}_i) < \underline{\delta}_i$, if $\boldsymbol{e}_i(0) < 0$ with $\bar{\delta}_i$ and $\underline{\delta}_i$ being positive constants satisfy $\underline{\delta}_i \leq \bar{\delta}_i$.
3)
$$\left.\begin{matrix}\lim\limits_{\mathcal{E}_i\to-\infty}\mathcal{Z}(\mathcal{E}_i) = -\underline{\delta}_i \\ \lim\limits_{\mathcal{E}_i\to+\infty}\mathcal{Z}(\mathcal{E}_i) = \bar{\delta}_i\end{matrix}\right\} \text{ if } \boldsymbol{e}_i \geq 0$$
$$\left.\begin{matrix}\lim\limits_{\mathcal{E}_i\to-\infty}\mathcal{Z}(\mathcal{E}_i) = -\bar{\delta}_i \\ \lim\limits_{\mathcal{E}_i\to+\infty}\mathcal{Z}(\mathcal{E}_i) = \underline{\delta}_i\end{matrix}\right\} \text{ if } \boldsymbol{e}_i < 0$$

such that

$$\mathcal{Z}(\mathcal{E}_i) = \begin{cases} \frac{\bar{\delta}_i\exp(\mathcal{E}_i) - \underline{\delta}_i\exp(-\mathcal{E}_i)}{\exp(\mathcal{E}_i)+\exp(-\mathcal{E}_i)}, & \bar{\delta}_i \geq \underline{\delta}_i \text{ if } \boldsymbol{e}_i \geq 0 \\ \frac{\underline{\delta}_i\exp(\mathcal{E}_i) - \bar{\delta}_i\exp(-\mathcal{E}_i)}{\exp(\mathcal{E}_i)+\exp(-\mathcal{E}_i)}, & \underline{\delta}_i \geq \bar{\delta}_i \text{ if } \boldsymbol{e}_i < 0. \end{cases} \tag{35}$$

The transformed error could be extracted through the inverse transformation of (35)

$$\mathcal{E}_i(\boldsymbol{e}_i, \xi_i) = \mathcal{Z}^{-1}(\boldsymbol{e}_i/\xi_i) \tag{36}$$

with $\mathcal{E}_i \in \mathbb{R}$, $\mathcal{Z} \in \mathbb{R}$, and $\mathcal{Z}^{-1} \in \mathbb{R}$ being smooth functions. For simplicity, let $\mathcal{E}_i \coloneqq \mathcal{E}_i(\cdot,\cdot)$, $\bar{\delta} = [\bar{\delta}_1, \bar{\delta}_2, \bar{\delta}_3, \bar{\delta}_4]^\top$, $\underline{\delta} = [\underline{\delta}_1, \underline{\delta}_2, \underline{\delta}_3, \underline{\delta}_4]^\top$, $\mathcal{E} = [\mathcal{E}_R, \mathcal{E}_P^\top]^\top$ for all $\bar{\delta}, \underline{\delta}, \mathcal{E} \in \mathbb{R}^4$ with $\mathcal{E}_R = \mathcal{E}_1 \in \mathbb{R}$ and $\mathcal{E}_P = [\mathcal{E}_2, \mathcal{E}_3, \mathcal{E}_4]^\top \in \mathbb{R}^3$. In fact, the transformed error $\mathcal{E}_i$ translates $\boldsymbol{e}_i$ from the given constrained form in (32) or (33) to its unconstrained form as in (36). From (35), the inverse transformation can be expressed as

$$\mathcal{E}_i = \frac{1}{2}\begin{cases} \ln\frac{\bar{\delta}_i+\boldsymbol{e}_i/\xi_i}{\bar{\delta}_i-\boldsymbol{e}_i/\xi_i}, & \bar{\delta}_i \geq \underline{\delta}_i \text{ if } \boldsymbol{e}_i \geq 0 \\ \ln\frac{\underline{\delta}_i+\boldsymbol{e}_i/\xi_i}{\underline{\delta}_i-\boldsymbol{e}_i/\xi_i}, & \underline{\delta}_i \geq \bar{\delta}_i \text{ if } \boldsymbol{e}_i < 0. \end{cases} \tag{37}$$

Remark 2: Consider the transformed error in (37). The transient and steady-state performance of the tracking error $(\boldsymbol{e}_i)$ is bounded by the performance function ξ_i, and therefore, the prescribed performance is achieved if and only if $\mathcal{E}_i$ is guaranteed to be bounded for all $t \geq 0$.

Proposition 1: Consider the error vector in (30) with the normalized Euclidean distance error $||\tilde{R}||_I$ being given by (4). From (34)–(36), let the transformed error be expressed as in (37) provided that $\underline{\delta} = \bar{\delta}$. Then the following statements are true.

1) The only possible representation of $\mathcal{E}_1$ is as follows:

$$\mathcal{E}_1 = \frac{1}{2}\ln\frac{\underline{\delta}_1+\boldsymbol{e}_1/\xi_1}{\bar{\delta}_1-\boldsymbol{e}_1/\xi_1} = \frac{1}{2}\ln\frac{\underline{\delta}_1+||\tilde{R}||_I/\xi_1}{\bar{\delta}_1-||\tilde{R}||_I/\xi_1}. \tag{38}$$

2) The transformed error $\mathcal{E}_1 > 0\ \forall ||\tilde{R}||_I \neq 0$.
3) $\mathcal{E} = \underline{\mathbf{0}}_4$ only at $\boldsymbol{e} = \underline{\mathbf{0}}_4$ and the critical point of $\mathcal{E}$ satisfies $\boldsymbol{e} = \underline{\mathbf{0}}_4$.
4) The only critical point of $\mathcal{E}$ is $\tilde{\boldsymbol{T}} = \mathbf{I}_4$.

Proof: Given that $0 \leq ||\tilde{R}(t)||_I \leq 1\ \forall t \geq 0$ as defined in (4), one can find that the upper part of (37) holds $\forall t \geq 0$ which proves 1). Since $\underline{\delta} = \bar{\delta}$ with the constraint $||\tilde{R}||_I \leq \xi_1$, the expression in (38) is $(\underline{\delta}_1 + ||\tilde{R}||_I/\xi_1)/(\bar{\delta}_1 - ||\tilde{R}||_I/\xi_1) \geq 1\ \forall ||\tilde{R}||_I \neq 0$. Thus, $\mathcal{E}_1 > 0\ \forall ||\tilde{R}||_I \neq 0$ which confirms 2). Considering $\underline{\delta} = \bar{\delta}$ with the constraint $\boldsymbol{e}_i \leq \xi_i$, it is clear that $(\underline{\delta}_i + \boldsymbol{e}_i/\xi_i)/(\bar{\delta}_i - \boldsymbol{e}_i/\xi_i) = 1$ if and only if $\boldsymbol{e}_i = 0$. Accordingly, $\mathcal{E}_i \neq 0\ \forall \boldsymbol{e}_i \neq 0$ and $\mathcal{E}_i = 0$ only at $\boldsymbol{e}_i = 0$ which proves 3). For 4), from (4) and (27), $||\tilde{R}||_I = 0$ and $\tilde{P} = 0$ if and only if $\tilde{\boldsymbol{T}} = \mathbf{I}_4$. Thus, the critical point of $\mathcal{E}$ satisfies $||\tilde{R}||_I = 0$ and $\tilde{P} = 0$ which in turn satisfies $\tilde{\boldsymbol{T}} = \mathbf{I}_4$ and proves 4). Define $\mu_i \coloneqq \mu_i(\boldsymbol{e}_i, \xi_i)$ such that

$$\mu_i = \frac{1}{2\xi_i}\frac{\partial \mathcal{Z}^{-1}(\boldsymbol{e}_i/\xi_i)}{\partial(\boldsymbol{e}_i/\xi_i)} = \frac{1}{2\xi_i}\left(\frac{1}{\underline{\delta}_i + \boldsymbol{e}_i/\xi_i} + \frac{1}{\bar{\delta}_i - \boldsymbol{e}_i/\xi_i}\right). \tag{39}$$

Hence, one can find that the derivative of $\dot{\mathcal{E}}_i$ is as follows:

$$\dot{\mathcal{E}}_i = \mu_i\left(\dot{\boldsymbol{e}}_i - \frac{\dot{\xi}_i}{\xi_i}\boldsymbol{e}_i\right). \tag{40}$$

More simply, the expression in (40) is

$$\dot{\mathcal{E}} = \begin{bmatrix} \boldsymbol{\Psi}_R & \underline{\mathbf{0}}_3^\top \\ \underline{\mathbf{0}}_3 & \boldsymbol{\Psi}_P \end{bmatrix}\left(\dot{\boldsymbol{e}} - \begin{bmatrix} \boldsymbol{\Lambda}_R & \underline{\mathbf{0}}_3^\top \\ \underline{\mathbf{0}}_3 & \boldsymbol{\Lambda}_P \end{bmatrix}\boldsymbol{e}\right) \tag{41}$$

with $\boldsymbol{\Lambda}_R = (\dot{\xi}_1/\xi_1)$, $\boldsymbol{\Lambda}_P = \text{diag}((\dot{\xi}_2/\xi_2), (\dot{\xi}_3/\xi_3), (\dot{\xi}_4/\xi_4))$, $\boldsymbol{\Psi}_R = \mu_1$, and $\boldsymbol{\Psi}_P = \text{diag}(\mu_2, \mu_3, \mu_4)$ for all $\boldsymbol{\Lambda}_R, \boldsymbol{\Psi}_R \in \mathbb{R}$, and $\boldsymbol{\Lambda}_P, \boldsymbol{\Psi}_P \in \mathbb{R}^{3\times 3}$. The following section introduces two nonlinear pose filters on $\mathbb{SE}(3)$ with prescribed performance characteristics which for $0 \leq |\boldsymbol{e}_i(0)| < \xi_i(0)$ guarantee $\mathcal{E}_i \in \mathcal{L}_\infty\ \forall t \geq 0$ and, therefore, satisfy (32) or (33). ■

IV. Nonlinear Complementary Pose Filters on $\mathbb{SE}(3)$ With Prescribed Performance

This section aims to provide a comprehensive description of the two nonlinear complementary pose filters evolved on $\mathbb{SE}(3)$ with the error vector, introduced in (30), behaving in accordance with the predefined transient as well as steady-state measures specified by the user. The first proposed filter is named a semi-direct pose filter (S-DIR) with prescribed performance and the second one is termed a direct pose filter with prescribed performance. The difference between the two lies in the fact that while the semi-direct filter requires both attitude and position to be reconstructed through a set of vectorial measurements given in (15) and (17) combined with the measurement of the group velocity vector as described in (22) and (23), the direct filter (DIR) only utilizes the above-mentioned measurements in the filter design. The structure of the proposed pose filters described in the two subsequent sections is nonlinear on the Lie group of $\mathbb{SE}(3)$ and is given by

$$\dot{\hat{\boldsymbol{T}}} = \hat{\boldsymbol{T}}[\hat{\mathcal{Y}}]_\wedge$$

with $\hat{\mathcal{Y}} = [\hat{\Omega}^\top, \hat{V}^\top] \in \mathbb{R}^6$ such that $\dot{\hat{R}} = \hat{R}[\hat{\Omega}]_\times$ and $\dot{\hat{P}} = \hat{R}\hat{V}$.

A. Semi-Direct Pose Filter With Prescribed Performance

Recall the error in (30) $\boldsymbol{e} = \left[||\tilde{R}||_I, \tilde{P}^\top\right]^\top$. Define $\boldsymbol{T}_y = \begin{bmatrix} R_y & P_y \\ \underline{\mathbf{0}}_3^\top & 1 \end{bmatrix}$ as a reconstructed homogeneous transformation matrix of the true $\boldsymbol{T}$. R_y corrupted by uncertain measurements can be reconstructed as in [1] and [2] or, for simplicity, see the Appendix in [3] and [13]. From (18) and (19), P_y is reconstructed in the following manner:

$$\begin{aligned} P_y &= \frac{1}{\sum_{i=1}^{N_L} k_i^L}\sum_{i=1}^{N_L} k_i^L\left(v_i^{\mathcal{I}(L)} - R_y v_i^{\mathcal{B}(L)}\right) \\ &= \mathcal{G}_c^{\mathcal{I}} - R_y\mathcal{G}_c^{\mathcal{B}}. \end{aligned} \tag{42}$$

Consider the following pose filter design:

$$\dot{\hat{R}} = \hat{R}\left[\Omega_m - \hat{b}_\Omega - \hat{R}^\top W_\Omega\right]_\times \tag{43}$$

$$\dot{\hat{P}} = \hat{R}(V_m - \hat{b}_V - W_V) \tag{44}$$

$$\begin{aligned} \dot{\hat{b}}_\Omega = {} & \frac{\gamma}{2}\boldsymbol{\Psi}_R\mathcal{E}_R\hat{R}^\top\mathbf{vex}(\boldsymbol{\mathcal{P}}_a(\tilde{R})) \\ & + \gamma\hat{R}^\top\left[\tilde{P} - \hat{P}\right]_\times\boldsymbol{\Psi}_P\mathcal{E}_P \end{aligned} \tag{45}$$

$$\dot{\hat{b}}_V = \gamma\hat{R}^\top\boldsymbol{\Psi}_P\mathcal{E}_P \tag{46}$$

$$W_\Omega = 2\frac{k_w\boldsymbol{\Psi}_R\mathcal{E}_R - \boldsymbol{\Lambda}_R/4}{1 - ||\tilde{R}||_I}\mathbf{vex}(\boldsymbol{\mathcal{P}}_a(\tilde{R})) \tag{47}$$

$$W_V = \hat{R}^\top\left(k_w\boldsymbol{\Psi}_P\mathcal{E}_P + \left[\tilde{P} - \hat{P}\right]_\times W_\Omega - \boldsymbol{\Lambda}_P\tilde{P}\right) \tag{48}$$

with $\tilde{R} = \hat{R}R_y^\top$, $\tilde{P} = \hat{P} - \tilde{R}P_y$, $\mathcal{E}_R$, $\mathcal{E}_P$, $\boldsymbol{\Psi}_R$, and $\boldsymbol{\Psi}_P$ being defined in (39) and (40), respectively, k_w and γ being positive constants, and each of $\hat{b}_\Omega$ and $\hat{b}_V$ being the estimates of b_Ω and b_V, respectively.

Define the error between the true and the estimated bias by

$$\tilde{b}_\Omega = b_\Omega - \hat{b}_\Omega \tag{49}$$

$$\tilde{b}_V = b_V - \hat{b}_V \tag{50}$$

where $\tilde{b} = \left[\tilde{b}_\Omega^\top, \tilde{b}_V^\top\right]^\top \in \mathbb{R}^6$ is the group error bias vector.

Theorem 1: Consider the pose dynamics in (21), the group of noise-free velocity measurements in (22) and (23) such that $\Omega_m = \Omega + b_\Omega$ and $V_m = V + b_V$, in addition to other vector measurements given in (15) and (17) coupled with the filter kinematics in (43)–(48). Let Assumption 1 holds. Define $\mathcal{U} \subseteq \mathbb{SE}(3) \times \mathbb{R}^6$ by $\mathcal{U} \coloneqq \{.(\tilde{\boldsymbol{T}}(0), \tilde{b}(0))|\text{Tr}\{\tilde{R}(0)\} = -1, \tilde{P}(0) = \underline{\mathbf{0}}_3, \tilde{b}(0) = \underline{\mathbf{0}}_6\}$. From almost any initial condition such that $\text{Tr}\{\tilde{R}(0)\} \notin \mathcal{U}$ and $\mathcal{E}(0) \in \mathcal{L}_\infty$, all signals in the closed-loop are bounded, $\lim_{t\to\infty}\mathcal{E}(t) = 0$, and $\tilde{\boldsymbol{T}}$ asymptotically approaches $\mathbf{I}_4$.

Theorem 1 guarantees that the observer pose dynamics in (43)–(48) are stable with $\mathcal{E}(t)$ asymptotically approaching the origin. Since $\mathcal{E}(t)$ is bounded, the error vector $\boldsymbol{e}$ in (30) is constrained by the transient and steady-state boundaries introduced in (31).

Proof: Consider the error in the homogeneous transformation matrix from body-frame to estimator-frame defined as (27). From (20) and (43), the error dynamics are

$$\dot{\tilde{R}} = \hat{R}\left[\tilde{b}_\Omega - \hat{R}^\top W_\Omega\right]_\times R^\top = \left[\hat{R}\tilde{b}_\Omega - W_\Omega\right]_\times\tilde{R} \tag{51}$$

where $[\hat{R}\tilde{b}_\Omega]_\times = \hat{R}[\tilde{b}_\Omega]_\times \hat{R}^\top$ as given in identity (7). In view of (20) and (24), one can express the error dynamics in (51) in terms of normalized Euclidean distance as

$$\begin{aligned}\frac{d}{dt}||\tilde{R}||_I &= \frac{d}{dt}\frac{1}{4}\mathrm{Tr}\{\mathbf{I}_3 - \tilde{R}\}\\ &= -\frac{1}{4}\mathrm{Tr}\left\{\left[\hat{R}\tilde{b}_\Omega - W_\Omega\right]_\times \boldsymbol{\mathcal{P}}_a(\tilde{R})\right\}\\ &= \frac{1}{2}\mathbf{vex}(\boldsymbol{\mathcal{P}}_a(\tilde{R}))^\top(\hat{R}\tilde{b}_\Omega - W_\Omega) \end{aligned} \tag{52}$$

with $\mathrm{Tr}\{\tilde{R}[\tilde{b} - W]_\times\} = -2\mathbf{vex}(\boldsymbol{\mathcal{P}}_a(\tilde{R}))^\top(\tilde{b} - W)$ being defined in (11). Since the position error is given by $\tilde{P} = \hat{P} - \tilde{R}P$ in (27), one can find the derivative of $\tilde{P}$ to be

$$\begin{aligned}\dot{\tilde{P}} &= \dot{\hat{P}} - \dot{\tilde{R}}P - \tilde{R}\dot{P}\\ &= \dot{\hat{P}} - \left[\hat{R}\tilde{b}_\Omega - W_\Omega\right]_\times \tilde{R}P - \tilde{R}R(V_m - b_V)\\ &= \hat{R}(\tilde{b}_V - W_V) + \left[\hat{P} - \tilde{P}\right]_\times \left(\hat{R}\tilde{b}_\Omega - W_\Omega\right)\end{aligned} \tag{53}$$

with $[\hat{R}\tilde{b}_\Omega]_\times \hat{P} = -[\hat{P}]_\times \hat{R}\tilde{b}_\Omega$. From (52) and (53), and in view of (25), the dynamics of the error vector in (30) become

$$\begin{bmatrix} ||\dot{\tilde{R}}||_I \\ \dot{\tilde{P}} \end{bmatrix} = \begin{bmatrix} \frac{1}{2}\mathbf{vex}(\boldsymbol{\mathcal{P}}_a(\tilde{R}))^\top & \mathbf{0}_3^\top \\ \left[\hat{P} - \tilde{P}\right]_\times & \hat{R} \end{bmatrix} \begin{bmatrix} \hat{R}\tilde{b}_\Omega - W_\Omega \\ \tilde{b}_V - W_V \end{bmatrix}. \tag{54}$$

Accordingly, the derivative of the transformed error in (41) can be represented with direct substitution of $\boldsymbol{e} = [||\tilde{R}||_I, \tilde{P}^\top]^\top$ in addition to the result in (54). Now, consider the following candidate Lyapunov function:

$$V\left(\mathcal{E}, \tilde{b}_\Omega, \tilde{b}_V\right) = \frac{1}{2}||\mathcal{E}||^2 + \frac{1}{2\gamma}||\tilde{b}_\Omega||^2 + \frac{1}{2\gamma}||\tilde{b}_V||^2. \tag{55}$$

Differentiating $V := V(\mathcal{E}, \tilde{b}_\Omega, \tilde{b}_V)$ in (55) results in

$$\begin{aligned}\dot{V} &= \mathcal{E}^\top\dot{\mathcal{E}} - \frac{1}{\gamma}\tilde{b}_\Omega^\top\dot{\hat{b}}_\Omega - \frac{1}{\gamma}\tilde{b}_V^\top\dot{\hat{b}}_V\\ &= \mathcal{E}_R\boldsymbol{\Psi}_R\left(\frac{1}{2}\mathbf{vex}\left(\boldsymbol{\mathcal{P}}_a(\tilde{R})\right)^\top\left(\hat{R}\tilde{b}_\Omega - W_\Omega\right) - \boldsymbol{\Lambda}_R||\tilde{R}||_I\right)\\ &\quad + \mathcal{E}_P^\top\boldsymbol{\Psi}_P\left(\hat{R}(\tilde{b}_V - W_V) + \left[\hat{P} - \tilde{P}\right]_\times\left(\hat{R}\tilde{b}_\Omega - W_\Omega\right)\right)\\ &\quad - \mathcal{E}_P^\top\boldsymbol{\Psi}_P\boldsymbol{\Lambda}_P\tilde{P} - \frac{1}{\gamma}\tilde{b}_\Omega^\top\dot{\hat{b}}_\Omega - \frac{1}{\gamma}\tilde{b}_V^\top\dot{\hat{b}}_V.\end{aligned} \tag{56}$$

Consider $||\tilde{R}||_I = (1/4)[(||\mathbf{vex}(\boldsymbol{\mathcal{P}}_a(\tilde{R}))||^2)/(1 - ||\tilde{R}||_I)]$ as defined in (28). Using the result in (56) and directly substituting $\dot{\hat{b}}_\Omega$, $\dot{\hat{b}}_V$, W_Ω, and W_V with their definitions in (45), (46), (47), and (48), respectively, one obtains

$$\begin{aligned}\dot{V} &= -\frac{1}{4}k_w\mathcal{E}_R^2\boldsymbol{\Psi}_R^2\frac{||\mathbf{vex}(\boldsymbol{\mathcal{P}}_a(\tilde{R}))||^2}{1 - ||\tilde{R}||_I} - k_w\mathcal{E}_P^\top\boldsymbol{\Psi}_P^2\mathcal{E}_P\\ &= -k_w\mathcal{E}_R^2\boldsymbol{\Psi}_R^2||\tilde{R}||_I - k_w\mathcal{E}_P^\top\boldsymbol{\Psi}_P^2\mathcal{E}_P.\end{aligned} \tag{57}$$

The result obtained in (57) indicates that $V(t) \leq V(0)\ \forall t \geq 0$. Given that $V(t) \leq V(0)\ \forall t \geq 0$, $\tilde{R}(0) \notin \mathcal{U}$ and $\mathcal{E}(0) \in \mathbb{R}^4$, $\tilde{b}$ remains bounded, and $\mathcal{E}$ is bounded and well defined for all $t \geq 0$. Consequently, $\tilde{P}$, $||\tilde{R}||_I$, and $\mathbf{vex}(\boldsymbol{\mathcal{P}}_a(\tilde{R}))$ are bounded, which in turn signifies that $\tilde{P}$, $||\dot{\tilde{R}}||_I$, $\dot{\mathcal{E}}_R$, and $\dot{\mathcal{E}}_P$ are bounded as well. From the result in (57) it follows that:

$$\begin{aligned}\ddot{V} &= -k_w\Big(2\mathcal{E}_R\boldsymbol{\Psi}_R\big(\dot{\mathcal{E}}_R\boldsymbol{\Psi}_R + \mathcal{E}_R\dot{\boldsymbol{\Psi}}_R\big)||\tilde{R}||_I + \mathcal{E}_R^2\boldsymbol{\Psi}_R^2||\dot{\tilde{R}}||_I\Big)\\ &\quad - 2k_w\mathcal{E}_P^\top\boldsymbol{\Psi}_P^2\dot{\mathcal{E}}_P - 2k_w\mathcal{E}_P^\top\boldsymbol{\Psi}_P\dot{\boldsymbol{\Psi}}_P\mathcal{E}_P.\end{aligned} \tag{58}$$

Since $\boldsymbol{\Psi}_R = \mu_1$ and $\boldsymbol{\Psi}_P = \mathrm{diag}(\mu_2, \mu_3, \mu_4)$ defined in (39), $\dot{\mu}_i$ can be expressed as follows for all $i = 1, 2, \ldots, 4$:

$$\dot{\mu}_i = -\frac{1}{2}\frac{\underline{\delta}_i\dot{\xi}_i + \dot{\boldsymbol{e}}_i}{(\underline{\delta}_i\xi_i + \boldsymbol{e}_i)^2} - \frac{1}{2}\frac{\bar{\delta}_i\dot{\xi}_i - \dot{\boldsymbol{e}}_i}{(\bar{\delta}_i\xi_i - \boldsymbol{e}_i)^2} \tag{59}$$

with $\dot{\xi}_i = -\ell_i(\xi_i^0 - \xi_i^\infty)\exp(-\ell_i t)$. Due to the fact that $\dot{\boldsymbol{e}}_i$ is bounded for all $i = 1, 2, \ldots, 4$, $\dot{\mu}_i$ is bounded and $\ddot{V}$ in (58) is uniformly bounded for all $t \geq 0$. It should be remarked that $\mathcal{E}_1 > 0$ for all $||\tilde{R}||_I > 0$, and $\mathcal{E}_1 \to 0$ as $||\tilde{R}||_I \to 0$ and vice versa as stated in property 2) of Proposition 1. In addition, $\mathcal{E}_i \neq 0\ \forall \boldsymbol{e}_i \neq 0$ and $\mathcal{E}_i = 0$ if and only if $\boldsymbol{e}_i = 0$ as indicated in property 3) of Proposition 1. Therefore, $\dot{V}$ is uniformly continuous, and in consistence with the Barbalat's lemma, $\dot{V} \to 0$ as $t \to \infty$ signifies that $\mathcal{E}_i \to 0$ and $\boldsymbol{e}_i \to 0$. As mentioned by property 4) of Proposition 1, $\mathcal{E} \to 0$ implies that $\tilde{\boldsymbol{T}}$ asymptotically approaches $\mathbf{I}_4$ which completes the proof. ■

B. Direct Pose Filter With Prescribed Performance

The reconstructed homogeneous transformation matrix $\boldsymbol{T}_y$ defined in Section IV-A consists of two elements: R_y and P_y. Although, R_y can be statically reconstructed applying, for example, QUEST [1] or SVD [2], the aforementioned methods of static reconstruction could significantly increase processing cost [7], [8], [29]. Thus, the pose filter proposed in this section avoids the necessity of attitude reconstruction and instead uses measurements from the inertial- and body-frame units directly. Let us define

$$\begin{aligned}\boldsymbol{\mathcal{M}}_T = \begin{bmatrix} \mathbf{M}_T & \mathbf{m}_v \\ \mathbf{m}_v^\top & \mathbf{m}_c \end{bmatrix} &= \sum_{i=1}^{N_R} k_i^R \begin{bmatrix} \upsilon_i^{\mathcal{I}(R)} \\ 0 \end{bmatrix}\begin{bmatrix} \upsilon_i^{\mathcal{I}(R)} \\ 0 \end{bmatrix}^\top\\ &\quad + \sum_{j=1}^{N_L} k_j^L \begin{bmatrix} \nu_j^{\mathcal{I}(L)} \\ 1 \end{bmatrix}\begin{bmatrix} \nu_j^{\mathcal{I}(L)} \\ 1 \end{bmatrix}^\top\end{aligned} \tag{60}$$

such that $\mathbf{M}_T = \mathbf{M}_R + \mathbf{M}_L$ with

$$\begin{aligned}\mathbf{M}_R &= \sum_{i=1}^{N_R} k_i^R \upsilon_i^{\mathcal{I}(R)}\left(\upsilon_i^{\mathcal{I}(R)}\right)^\top\\ \mathbf{M}_L &= \sum_{j=1}^{N_L} k_j^L \nu_j^{\mathcal{I}(L)}\left(\nu_j^{\mathcal{I}(L)}\right)^\top\\ \mathbf{m}_v &= \sum_{j=1}^{N_L} k_j^L \nu_j^{\mathcal{I}(L)}\\ \mathbf{m}_c &= \sum_{j=1}^{N_L} k_j^L\end{aligned} \tag{61}$$

where k_i^R and k_j^L are constant gains of the confidence level of ith and jth sensor measurements, respectively. Define

$$\begin{aligned}\boldsymbol{\mathcal{K}}_T = \begin{bmatrix} \mathbf{K}_T & \mathbf{k}_v \\ \mathbf{m}_v^\top & \mathbf{m}_c \end{bmatrix} &= \sum_{i=1}^{N_R} k_i^R \begin{bmatrix} \upsilon_i^{\mathcal{B}(R)} \\ 0 \end{bmatrix}\begin{bmatrix} \upsilon_i^{\mathcal{I}(R)} \\ 0 \end{bmatrix}^\top\\ &\quad + \sum_{j=1}^{N_L} k_j^L \begin{bmatrix} \nu_j^{\mathcal{B}(L)} \\ 1 \end{bmatrix}\begin{bmatrix} \nu_j^{\mathcal{I}(L)} \\ 1 \end{bmatrix}^\top\end{aligned} \tag{62}$$

such that $\mathbf{m}_v = \sum_{j=1}^{N_L} k_j^L v_j^{\mathcal{I}(L)}$ and $\mathbf{m}_c = \sum_{j=1}^{N_L} k_j^L$ as defined in (61), and

$$\mathbf{K}_T = \sum_{i=1}^{N_R} k_i^R \upsilon_i^{\mathcal{B}(R)} \left(\upsilon_i^{\mathcal{I}(R)}\right)^\top + \sum_{j=1}^{N_L} k_i^L v_j^{\mathcal{B}(L)} \left(v_j^{\mathcal{I}(L)}\right)^\top$$
$$\mathbf{k}_v = \sum_{j=1}^{N_L} k_j^L v_j^{\mathcal{B}(L)}. \tag{63}$$

In this paper, k_i^R is selected such that $\sum_{i=1}^{N_R} k_i^R = 3$. It can be easily deduced that $\mathbf{M}_R$ is symmetric. Assuming that Assumption 1 holds, $\mathbf{M}_R$ is nonsingular with $\text{rank}(\mathbf{M}_R) = 3$. Accordingly, the three eigenvalues of $\mathbf{M}_R$ are greater than zero. Define $\bar{\mathbf{M}}_R = \text{Tr}\{\mathbf{M}_R\}\mathbf{I}_3 - \mathbf{M}_R \in \mathbb{R}^{3\times 3}$, provided that $\text{rank}(\mathbf{M}_R) = 3$, then, the following three statements hold ([30, p. 553]).

1) $\mathbf{M}_R$ is a positive-definite matrix.
2) The eigenvectors of $\mathbf{M}_R$ coincide with the eigenvectors of $\bar{\mathbf{M}}_R$.
3) Assuming that the three eigenvalues of $\mathbf{M}_R$ are $\lambda(\mathbf{M}_R) = \{\lambda_1, \lambda_2, \lambda_3\}$, then $\lambda(\bar{\mathbf{M}}_R) = \{\lambda_3 + \lambda_2, \lambda_3 + \lambda_1, \lambda_2 + \lambda_1\}$ with the minimum singular value $\underline{\lambda}(\bar{\mathbf{M}}_R) > 0$.

In the remainder of this section, it is considered that $\text{rank}(\mathbf{M}_R) = 3$ in order to ensure that the above-mentioned statements are true. Define

$$\hat{\upsilon}_i^{\mathcal{B}(R)} = \hat{R}^\top \upsilon_i^{\mathcal{I}(R)}. \tag{64}$$

Defining the error in the homogeneous transformation matrix as in (27), the attitude error can be expressed as $\tilde{R} = \hat{R}R^\top$ and the position error is defined by $\tilde{P} = \hat{P} - \tilde{R}P$. Also, let the bias error be as in (49) and (50). In order to derive the direct pose filter, it is necessary to introduce the following series of equations written in terms of vectorial measurements. According to identity (6) and (7), one has

$$\begin{aligned}
&\left[\hat{R}\sum_{i=1}^{N_R} \frac{k_i^R}{2} \hat{\upsilon}_i^{\mathcal{B}(R)} \times \upsilon_i^{\mathcal{B}(R)}\right]_\times \\
&= \hat{R}\left[\sum_{i=1}^{N_R} \frac{k_i^R}{2} \hat{\upsilon}_i^{\mathcal{B}(R)} \times \upsilon_i^{\mathcal{B}(R)}\right]_\times \hat{R}^\top \\
&= \hat{R}\sum_{i=1}^{N_R} \frac{k_i^R}{2}\left(\upsilon_i^{\mathcal{B}(R)}\left(\hat{\upsilon}_i^{\mathcal{B}(R)}\right)^\top - \hat{\upsilon}_i^{\mathcal{B}(R)}\left(\upsilon_i^{\mathcal{B}(R)}\right)^\top\right)\hat{R}^\top \\
&= \frac{1}{2}\hat{R}R^\top\mathbf{M}_R - \frac{1}{2}\mathbf{M}_R R\hat{R}^\top \\
&= \mathcal{P}_a\big(\tilde{R}\mathbf{M}_R\big)
\end{aligned}$$

such that

$$\mathbf{vex}(\mathcal{P}_a(\tilde{R}\mathbf{M}_R)) = \hat{R}\sum_{i=1}^{N_R}\left(\frac{k_i^R}{2}\hat{\upsilon}_i^{\mathcal{B}(R)} \times \upsilon_i^{\mathcal{B}(R)}\right). \tag{65}$$

Thus, $\tilde{R}\mathbf{M}_R$ is defined in terms of vectorial measurements by

$$\tilde{R}\mathbf{M}_R = \hat{R}\sum_{i=1}^{N_R}\left(k_i^R \upsilon_i^{\mathcal{B}(R)}\left(\upsilon_i^{\mathcal{I}(R)}\right)^\top\right). \tag{66}$$

The normalized Euclidean distance of $\tilde{R}\mathbf{M}_R$ is found to be

$$\begin{aligned}
||\tilde{R}\mathbf{M}_R||_I &= \frac{1}{4}Tr\{(\mathbf{I}_3 - \tilde{R})\mathbf{M}_R\} \\
&= \frac{1}{4}\text{Tr}\left\{\mathbf{I}_3 - \hat{R}\sum_{i=1}^{N_R}\left(k_i^R \upsilon_i^{\mathcal{B}(R)}\left(\upsilon_i^{\mathcal{I}(R)}\right)^\top\right)\right\} \\
&= \frac{1}{4}\sum_{i=1}^{N_R}\left(1 - \left(\hat{\upsilon}_i^{\mathcal{B}(R)}\right)^\top \upsilon_i^{\mathcal{B}(R)}\right).
\end{aligned} \tag{67}$$

Let us introduce the following variable:

$$\begin{aligned}
\boldsymbol{\Upsilon}(\mathbf{M}_R, \tilde{R}) &= \text{Tr}\left\{\tilde{R}\mathbf{M}_R\mathbf{M}_R^{-1}\right\} \\
&= \text{Tr}\left\{\left(\sum_{i=1}^{N_R} k_i^R \upsilon_i^{\mathcal{B}(R)}\left(\upsilon_i^{\mathcal{I}(R)}\right)^\top\right)\right. \\
&\qquad \left.\bullet\left(\sum_{i=1}^{N_R} k_i^R \hat{\upsilon}_i^{\mathcal{B}(R)}\left(\upsilon_i^{\mathcal{I}(R)}\right)^\top\right)^{-1}\right\}
\end{aligned} \tag{68}$$

where $\bullet$ is a multiplication operator of the two matrices. From (60) and (61), one obtains

$$\tilde{\boldsymbol{T}}\boldsymbol{\mathcal{M}}^{\mathcal{I}} = \begin{bmatrix} \tilde{R}\mathbf{M}_T + \tilde{P}\mathbf{m}_v^\top & \tilde{R}\mathbf{m}_v + \mathbf{m}_c\tilde{P} \\ \mathbf{m}_v^\top & \mathbf{m}_c. \end{bmatrix} \tag{69}$$

The above-mentioned result can be additionally expressed as

$$\begin{aligned}
\tilde{\boldsymbol{T}}\boldsymbol{\mathcal{M}}^{\mathcal{I}} &= \begin{bmatrix} \hat{R} & \hat{P} \\ \mathbf{0}_3^\top & 1 \end{bmatrix}\begin{bmatrix} \mathbf{K}_T & \mathbf{k}_v \\ \mathbf{m}_v^\top & \mathbf{m}_c \end{bmatrix} \\
&= \begin{bmatrix} \hat{R}\mathbf{K}_T + \hat{P}\mathbf{m}_v^\top & \hat{R}\mathbf{k}_v + \mathbf{m}_c\hat{P} \\ \mathbf{m}_v^\top & \mathbf{m}_c. \end{bmatrix}.
\end{aligned} \tag{70}$$

As such, from (69) and (70), the position error can be reformulated with respect to vectorial measurements as

$$\tilde{P} = \hat{P} + \frac{1}{\mathbf{m}_c}\left(\hat{R}\mathbf{k}_v - \tilde{R}\mathbf{M}_R\mathbf{M}_R^{-1}\mathbf{m}_v\right) \tag{71}$$

with $\tilde{R}\mathbf{M}_R$ being calculated as in (66) and $\mathbf{m}_c \neq 0$ for at least one landmark. Consequently, $\mathbf{vex}(\mathcal{P}_a(\tilde{R}\mathbf{M}_R))$, $\tilde{R}\mathbf{M}_R$, $||\tilde{R}\mathbf{M}_R||_I$, $\boldsymbol{\Upsilon}(\mathbf{M}_R, \tilde{R})$, and $\tilde{P}$ will be obtained through a set of vectorial measurements as defined in (65), (66), (67), (68), and (71), respectively, in all the subsequent derivations and calculations. Let us modify the vector error in (30) to be

$$\boldsymbol{e} = [\boldsymbol{e}_1, \boldsymbol{e}_2, \boldsymbol{e}_3, \boldsymbol{e}_4]^\top = \left[||\tilde{R}\mathbf{M}_R||_I, \tilde{P}^\top\right]^\top \tag{72}$$

with $||\tilde{R}\mathbf{M}_R||_I$ and $\tilde{P}$ being defined in (67) and (71), respectively. Thus, all the discussion in Section III-B is to be reformulated using the error vector in (72) instead of (30). Define the minimum eigenvalue of $\bar{\mathbf{M}}_R$ as $\underline{\lambda} \coloneqq \underline{\lambda}(\bar{\mathbf{M}}_R)$, and consider the following filter design:

$$\dot{\hat{R}} = \hat{R}\Big[\Omega_m - \hat{b}_\Omega - \hat{R}^\top W_\Omega\Big]_\times \tag{73}$$
$$\dot{\hat{P}} = \hat{R}(V_m - \hat{b}_V - W_V) \tag{74}$$
$$\begin{aligned}
\dot{\hat{b}}_\Omega &= \frac{\gamma}{2}\boldsymbol{\Psi}_R\mathcal{E}_R\hat{R}^\top\mathbf{vex}\big(\mathcal{P}_a(\tilde{R}\mathbf{M}_R)\big) \\
&\quad + \gamma\hat{R}^\top\Big[\tilde{P} - \hat{P}\Big]_\times\boldsymbol{\Psi}_P\mathcal{E}_P
\end{aligned} \tag{75}$$
$$\dot{\hat{b}}_V = \gamma\hat{R}^\top\boldsymbol{\Psi}_P\mathcal{E}_P \tag{76}$$

$$W_\Omega = \frac{4}{\underline{\lambda}}\frac{k_w \boldsymbol{\Psi}_R \mathcal{E}_R - \boldsymbol{\Lambda}_R}{1+\boldsymbol{\Upsilon}(\mathbf{M}_R,\tilde{R})}\mathbf{vex}\big(\boldsymbol{\mathcal{P}}_a(\tilde{R}\mathbf{M}_R)\big) \tag{77}$$

$$W_V = \hat{R}^\top\left(k_w \boldsymbol{\Psi}_P \mathcal{E}_P + \Big[\tilde{P}-\hat{P}\Big]_\times W_\Omega - \boldsymbol{\Lambda}_P \tilde{P}\right) \tag{78}$$

with $\boldsymbol{\Upsilon}(\mathbf{M}_R,\tilde{R})$ and $\mathbf{vex}(\boldsymbol{\mathcal{P}}_a(\tilde{R}\mathbf{M}_R))$ being specified in (68) and (65), respectively, $\mathcal{E} = [\mathcal{E}_R, \mathcal{E}_P^\top]^\top = [\mathcal{E}_1, \mathcal{E}_2, \mathcal{E}_3, \mathcal{E}_4]^\top$, $\mathcal{E}_i \coloneqq \mathcal{E}_i(\boldsymbol{e}_i, \xi_i)$ and $\mu_i \coloneqq \mu_i(\boldsymbol{e}_i, \xi_i)$ being defined in (38) and (39), respectively, while $\boldsymbol{e}$ is as in (72), k_w and γ are positive constants, and $\hat{b}_\Omega$ and $\hat{b}_V$ are the estimates of b_Ω and b_V, respectively.

Theorem 2: Consider coupling the pose filter in (73)–(78) with the set of vector measurements in (15) and (17), and the velocity measurements in (22) and (23) where $\Omega_m = \Omega + b_\Omega$ and $V_m = V + b_V$. Let Assumption 1 holds. Define $\mathcal{U} \subseteq \mathbb{SE}(3)\times\mathbb{R}^6$ by $\mathcal{U} \coloneqq \{.(\tilde{\boldsymbol{T}}(0), \tilde{b}(0)) | \mathrm{Tr}\{\tilde{R}(0)\} = -1, \tilde{P}(0) = \underline{\mathbf{0}}_3, \tilde{b}(0) = \underline{\mathbf{0}}_6\}$. If $\tilde{R}(0) \notin \mathcal{U}$ and $\mathcal{E}(0) \in \mathcal{L}_\infty$, then, all error signals are bounded, $\mathcal{E}(t)$ asymptotically approaches 0, and $\tilde{\boldsymbol{T}}$ asymptotically approaches $\mathbf{I}_4$.

Theorem 2 guarantees the observer dynamics in (73)–(78) to be stable. In consistence with Remark 2, boundedness of $\mathcal{E}(t)$ indicates that $\boldsymbol{e}$ follows the dynamic decreasing boundaries in (31).

Proof: Consider the error in the homogeneous transformation matrix and bias defined as in (27), (49), and (50), respectively. From (20) and (73), the error dynamics of $\tilde{R}$ can be found to be analogous to (51). The ith inertial measurements $v_i^{\mathcal{I}(R)}$ and $v_i^{\mathcal{I}(L)}$ are constant, thus, $\dot{\mathbf{M}}_R = \mathbf{0}_{3\times3}$. Consequently, from (51), the derivative of $||\tilde{R}\mathbf{M}_R||_I$ is equivalent to

$$\begin{aligned}\frac{d}{dt}||\tilde{R}\mathbf{M}_R||_I &= -\frac{1}{4}\mathrm{Tr}\left\{\Big[\hat{R}\tilde{b}_\Omega - W_\Omega\Big]_\times \tilde{R}\mathbf{M}_R\right\}\\ &= -\frac{1}{4}\mathrm{Tr}\left\{\Big[\hat{R}\tilde{b}_\Omega - W_\Omega\Big]_\times \boldsymbol{\mathcal{P}}_a(\tilde{R}\mathbf{M}_R)\right\}\\ &= \frac{1}{2}\mathbf{vex}\big(\boldsymbol{\mathcal{P}}_a(\tilde{R}\mathbf{M}_R)\big)^\top\Big(\hat{R}\tilde{b}_\Omega - W_\Omega\Big)\end{aligned} \tag{79}$$

where $\mathrm{Tr}\{[W_\Omega]_\times \tilde{R}\mathbf{M}_R\} = -2\mathbf{vex}(\boldsymbol{\mathcal{P}}_a(\tilde{R}\mathbf{M}_R))^\top W_\Omega$ as given in (11). One could find that the derivative of $\tilde{P}$ is equivalent to (53). From (79) and (53), and in view of (25), the derivative of $\boldsymbol{e}$ given in (72), becomes

$$\dot{\boldsymbol{e}} = \begin{bmatrix}\frac{1}{2}\mathbf{vex}(\boldsymbol{\mathcal{P}}_a(\tilde{R}\mathbf{M}_R))^\top & 0_{1\times3}\\ \Big[\hat{P}-\tilde{P}\Big]_\times & \hat{R}\end{bmatrix}\begin{bmatrix}\hat{R}\tilde{b}_\Omega - W_\Omega\\ \tilde{b}_V - W_V\end{bmatrix}. \tag{80}$$

The derivative of the transformed error in (41) be acquired by direct substitution of $\boldsymbol{e}$ as in (72), in addition to the result in (80). Consider the candidate Lyapunov function

$$V\Big(\mathcal{E}, \tilde{b}_\Omega, \tilde{b}_V\Big) = \frac{1}{2}||\mathcal{E}||^2 + \frac{1}{2\gamma}||\tilde{b}_\Omega||^2 + \frac{1}{2\gamma}||\tilde{b}_V||^2. \tag{81}$$

The derivative of $V \coloneqq V(\mathcal{E}, \tilde{b}_\Omega, \tilde{b}_V)$ is as follows:

$$\begin{aligned}\dot{V} &= \mathcal{E}^\top\dot{\mathcal{E}} - \frac{1}{\gamma}\tilde{b}_\Omega^\top\dot{\hat{b}}_\Omega - \frac{1}{\gamma}\tilde{b}_V^\top\dot{\hat{b}}_V\\ &= \frac{1}{2}\mathcal{E}_R\boldsymbol{\Psi}_R\mathbf{vex}\big(\boldsymbol{\mathcal{P}}_a(\tilde{R}\mathbf{M}_R)\big)^\top\Big(\hat{R}\tilde{b}_\Omega - W_\Omega\Big)\\ &\quad + \mathcal{E}_P^\top\boldsymbol{\Psi}_P\left(\hat{R}(\tilde{b}_V - W_V) + \Big[\hat{P}-\tilde{P}\Big]_\times\Big(\hat{R}\tilde{b}_\Omega - W_\Omega\Big)\right)\\ &\quad - \mathcal{E}_R\boldsymbol{\Psi}_R\boldsymbol{\Lambda}_R||\tilde{R}\mathbf{M}_R||_I - \mathcal{E}_P^\top\boldsymbol{\Psi}_P\boldsymbol{\Lambda}_P\tilde{P}\\ &\quad - \frac{1}{\gamma}\tilde{b}_\Omega^\top\dot{\hat{b}}_\Omega - \frac{1}{\gamma}\tilde{b}_V^\top\dot{\hat{b}}_V.\end{aligned} \tag{82}$$

Directly substituting for $\dot{\hat{b}}_\Omega$, $\dot{\hat{b}}_V$, W_Ω, and W_V in (75), (76), (77), and (78), respectively, results in

$$\begin{aligned}\dot{V} \le{}& \boldsymbol{\Lambda}_R\left(\frac{2}{\underline{\lambda}}\frac{||\mathbf{vex}\big(\boldsymbol{\mathcal{P}}_a(\tilde{R}\mathbf{M}_R)\big)||^2}{1+\boldsymbol{\Upsilon}\big(\mathbf{M}_R,\tilde{R}\big)} - ||\tilde{R}\mathbf{M}_R||_I\right)\mathcal{E}_R\boldsymbol{\Psi}_R\\ &- \frac{2}{\underline{\lambda}}\frac{k_w\mathcal{E}_R^2\boldsymbol{\Psi}_R^2}{1+\boldsymbol{\Upsilon}\big(\mathbf{M}_R,\tilde{R}\big)}\big\|\mathbf{vex}\big(\boldsymbol{\mathcal{P}}_a(\tilde{R}\mathbf{M}_R)\big)\big\|^2\\ &- k_w\mathcal{E}_P^\top\boldsymbol{\Psi}_P^2\mathcal{E}_P.\end{aligned} \tag{83}$$

It can be easily found that

$$\boldsymbol{\Lambda}_R\left(\frac{2}{\underline{\lambda}}\frac{\big\|\mathbf{vex}\big(\boldsymbol{\mathcal{P}}_a(\tilde{R}\mathbf{M}_R)\big)\big\|^2}{1+\boldsymbol{\Upsilon}(\mathbf{M}_R,\tilde{R})} - ||\tilde{R}\mathbf{M}_R||_I\right)\mathcal{E}_R\boldsymbol{\Psi}_R \le 0 \tag{84}$$

where $\mathcal{E}_R > 0\ \forall||\tilde{R}\mathbf{M}_R||_I \neq 0$ and $\mathcal{E}_R = 0$ at $||\tilde{R}\mathbf{M}_R||_I = 0$ as presented in property 2) of Proposition 1, and $\boldsymbol{\Psi}_R > 0\ \forall t \ge 0$ as given in (39). Also, $\dot{\xi}_i$ is negative and strictly increasing that satisfies $\dot{\xi}_i \to 0$ as $t \to \infty$, and $\xi_i : \mathbb{R}_+ \to \mathbb{R}_+$ such that $\xi_i \to \xi_i^\infty$ as $t \to \infty$. Thus, $\dot{\xi}_i/\xi_i \le 0$ which means that $\boldsymbol{\Lambda}_R \le 0$. Considering (29) in Lemma 1, thus, the expression in (84) is negative semi-definite. As such, the inequality in (83) can be expressed as

$$\dot{V} \le -k_w\mathcal{E}_R^2\boldsymbol{\Psi}_R^2||\tilde{R}\mathbf{M}_R||_I - k_w\mathcal{E}_P^\top\boldsymbol{\Psi}_P^2\mathcal{E}_P. \tag{85}$$

This signifies that $V(t) \le V(0)\ \forall t \ge 0$. From almost any initial conditions such that $\mathrm{Tr}\{\tilde{R}(0)\} \neq -1$ and $\mathcal{E}(0) \in \mathbb{R}^4$, $\mathcal{E}$ and $\tilde{b}$ are bounded for all $t \ge 0$. Thereby, $\mathcal{E}$ is bounded and well-defined for all $t \ge 0$. $\tilde{P}$, $||\tilde{R}\mathbf{M}_R||_I$, and $\mathbf{vex}(\boldsymbol{\mathcal{P}}_a(\tilde{R}\mathbf{M}_R))$ are also bounded which indicates that $\tilde{P}$, $||\dot{\tilde{R}}\mathbf{M}_R||_I$, $\dot{\mathcal{E}}_R$, and $\dot{\mathcal{E}}_P$ are bounded as well. In order to prove asymptotic convergence of $\mathcal{E}$ to the origin and $\tilde{\boldsymbol{T}}$ to the identity, it is necessary to show that the second derivative of (81) is

$$\begin{aligned}\ddot{V} \le{}& -2k_w\mathcal{E}_R\boldsymbol{\Psi}_R\big(\dot{\mathcal{E}}_R\boldsymbol{\Psi}_R + \mathcal{E}_R\dot{\boldsymbol{\Psi}}_R\big)||\tilde{R}\mathbf{M}_R||_I\\ &- k_w\mathcal{E}_R^2\boldsymbol{\Psi}_R^2||\dot{\tilde{R}}\mathbf{M}_R||_I\\ &- 2k_w\mathcal{E}_P^\top\boldsymbol{\Psi}_P\big(\boldsymbol{\Psi}_P\dot{\mathcal{E}}_P + \dot{\boldsymbol{\Psi}}_P\mathcal{E}_P\big).\end{aligned} \tag{86}$$

Recall that $\boldsymbol{\Psi}_R = \mu_1$ and $\boldsymbol{\Psi}_P = \mathrm{diag}(\mu_2, \mu_3, \mu_4)$, where $\dot{\mu}_i$ was defined in (59) for all $i = 1, 2, \ldots, 4$. Since $\dot{\boldsymbol{e}}_i$ is bounded, $\dot{\mu}_i$ is bounded as well and $\ddot{V}$ in (86) is bounded for all $t \ge 0$. From property 2) of Proposition 1, $||\mathcal{E}_1|| \to 0$ indicates that $||\tilde{R}\mathbf{M}_R||_I \to 0$, while $\mathcal{E}_1 \neq 0\ \forall||\tilde{R}\mathbf{M}_R||_I \neq 0$ and according to property 3) of Proposition 1, $\mathcal{E}_i \neq 0\ \forall\boldsymbol{e}_i \neq 0$ and $\mathcal{E}_i = 0$ if and only if $\boldsymbol{e}_i = 0$ for all $i = 1, \ldots, 4$. Therefore, $\dot{V}$ is uniformly continuous, and on the basis of the Barbalat's lemma, $\dot{V} \to 0$ implies that $||\mathcal{E}|| \to 0$ and $\|\boldsymbol{e}\| \to 0$ as $t \to \infty$. This means that $\tilde{\boldsymbol{T}}$ approaches $\mathbf{I}_4$ asymptotically in accordance with property 4) of Proposition 1, which completes the proof. ■

The estimates $\dot{\hat{b}}_\Omega$ and $\dot{\hat{b}}_V$ and the correction factors W_Ω and W_V are the functions of the transformed error $\mathcal{E}$ and the auxiliary component μ. $\mathcal{E}$ and μ rely on the error $\boldsymbol{e}$ such that their values become increasingly aggressive as $||\tilde{R}||_I$ approaches the unstable equilibria $||\tilde{R}||_I \to +1$ and $\tilde{P} \to \infty$. Their dynamic behavior is essential for forcing the proposed filters to obey the prescribed performance constraints. On the other side, $\mathcal{E} \to 0$ as $\boldsymbol{e} \to 0$. This significant advantage was not offered in literature, such as [11]–[16].

Remark 3 (Design Parameters): The dynamic boundaries of $\boldsymbol{e}$ are described by $\bar{\delta}$, $\underline{\delta}$, ξ_∞, and ξ_0 where ξ_0 and ξ_∞ define the large and small sets, respectively. The rate of convergence from the given large set to the small set is controlled by ℓ. The initial value of $\boldsymbol{e}(0)$ in (30) or (72) can be easily obtained. When applying S-DIR, $R_y(0)$ can be reconstructed, for example, using [1] and [2] or, for simplicity, see the Appendix in [3], $P_y(0)$ can be evaluated by $P_y(0) = \mathcal{G}_c^{\mathcal{I}} - R_y(0)\mathcal{G}_c^{\mathcal{B}}$ as in (42) and, finally, $||\tilde{R}(0)||_I = (1/4)\text{Tr}\{\mathbf{I}_3 - \hat{R}(0)R_y^\top(0)\}$ and $\tilde{P}(0) = \hat{P}(0) - \tilde{R}(0)P_y(0)$. In case when the direct pose filter is used, $||\tilde{R}(0)\mathbf{M}_R||_I$ can be defined from (67) and $\tilde{P}(0)$ can be easily obtained in the form of a vectorial measurement based on (71). Next, the user can select $\bar{\delta}$, $\underline{\delta}$, and ξ_0 to be greater than $\boldsymbol{e}(0)$.

C. Simplified Steps of the Proposed Pose Filters

The implementation of the proposed nonlinear pose filters on $\mathbb{SE}(3)$ with prescribed performance given in Sections IV-A and IV-B can be summarized in the following seven simplified steps.

Step 1: Select $\gamma, k_w > 0$, $\bar{\delta} = \underline{\delta} > \boldsymbol{e}(0)$, the desired speed of the convergence rate ℓ, and the upper bound of the small set ξ_∞.

Step 2: For the case of the S-DIR, define $\boldsymbol{e} = [||\tilde{R}||_I, \tilde{P}^\top]^\top$ with $\tilde{R} = \hat{R}R_y^\top$ and $\tilde{P} = \hat{P} - \tilde{R}P_y$, where P_y is given in (42) and R_y is reconstructed (e.g., [1] and [2]). For the case of the direct pose filter, define $\boldsymbol{e} = [||\tilde{R}\mathbf{M}_R||_I, \tilde{P}^\top]^\top$ with $||\tilde{R}\mathbf{M}_R||_I$ and $\tilde{P}$ being specified as in (67) and (71), respectively.

Step 3: For the case of the S-DIR, evaluate $\mathbf{vex}(\boldsymbol{\mathcal{P}}_a(\tilde{R}))$, whereas, for the case of the direct pose filter, define $\mathbf{vex}(\boldsymbol{\mathcal{P}}_a(M^{\mathcal{B}}\tilde{R}))$ and $\boldsymbol{\Upsilon}(\mathbf{M}_R, \tilde{R})$ from (65) and (68), respectively.

Step 4: Find the PPF ξ from (31).

Step 5: Evaluate the transformed error $\mathcal{E}$, $\boldsymbol{\Lambda}_R$, $\boldsymbol{\Psi}_R$, $\boldsymbol{\Lambda}_P$, and $\boldsymbol{\Psi}_P$ from (38) and (39), respectively.

Step 6: Obtain the filter kinematics $\dot{\hat{R}}$, $\dot{\hat{P}}$, $\dot{\hat{b}}_\Omega$, $\dot{\hat{b}}_V$, W_Ω, and W_V from (43), (44), (45), (46), (47), and (48), respectively, for the S-DIR, or from (73), (74), (75), (76), (77), and (78), respectively, for the direct pose filter.

Step 7: Go to step 2.

V. Simulations

This section illustrates the robustness of the proposed pose filters on $\mathbb{SE}(3)$ with prescribed performance against large error in initialization of $\tilde{\boldsymbol{T}}(0)$ and high levels of bias and noise inherent to the measurement process. Let the dynamics of the homogeneous transformation matrix $\boldsymbol{T}$ follow (21). Define the true angular velocity (rad/s) by

$$\Omega = \left[\sin(0.5t), 0.7\sin(0.4t + \pi), 0.5\sin\left(0.35t + \frac{\pi}{3}\right)\right]^\top$$

with $R(0) = \mathbf{I}_3$. Consider the following true translational velocity (m/s):

$$V = \left[0.3\sin(0.6t), 0.18\sin\left(0.4t + \frac{\pi}{2}\right), 0.3\sin\left(0.1t + \frac{\pi}{4}\right)\right]^\top$$

and the initial position $P(0) = \underline{\mathbf{0}}_3$. Let the measurements of angular and translational velocities be $\Omega_m = \Omega + b_\Omega + \omega_\Omega$ and $V_m = V + b_V + \omega_V$, respectively, with $b_\Omega = 0.1[1, -1, 1]^\top$ and $b_V = 0.1[2, 5, 1]^\top$. ω_Ω and ω_V represent the random noise process at each time instant with zero mean and standard deviation (STD) equal to 0.15(rad/s) and 0.3(m/s), respectively. Assume that one landmark is available for measurement ($N_L = 1$)

$$v_1^{\mathcal{I}(L)} = \left[\frac{1}{2}, \sqrt{2}, 1\right]^\top$$

where the body-frame measurements are defined as (16) such that $v_1^{\mathcal{B}(L)} = R^\top(v_1^{\mathcal{I}(L)} - P) + b_1^{\mathcal{B}(L)} + \omega_1^{\mathcal{B}(L)}$. The bias vector is $b_1^{\mathcal{B}(L)} = 0.1[0.3, 0.2, -0.2]^\top$ while $\omega_1^{\mathcal{B}(L)}$ is a Gaussian noise vector with zero mean and STD $= 0.1$. Assume that two noncollinear inertial-frame vectors ($N_R = 2$) are available with

$$v_1^{\mathcal{I}(R)} = \frac{1}{\sqrt{3}}[1, -1, 1]^\top, v_2^{\mathcal{I}(R)} = [0, 0, 1]^\top$$

while the two body-frame vectors are defined as in (13) $v_i^{\mathcal{B}(R)} = R^\top v_i^{\mathcal{I}(R)} + b_i^{\mathcal{B}(R)} + \omega_i^{\mathcal{B}(R)}$ for $i = 1, 2$ such that $b_1^{\mathcal{B}(R)} = 0.1[-1, 1, 0.5]^\top$ and $b_2^{\mathcal{B}(R)} = 0.1[0, 0, 1]^\top$. In addition, $\omega_1^{\mathcal{B}(R)}$ and $\omega_2^{\mathcal{B}(R)}$ are the Gaussian noise vectors with zero mean and STD $= 0.1$. The third vector is obtained using $v_3^{\mathcal{I}(R)} = v_1^{\mathcal{I}(R)} \times v_2^{\mathcal{I}(R)}$ and $v_3^{\mathcal{B}(R)} = v_1^{\mathcal{B}(R)} \times v_2^{\mathcal{B}(R)}$. This step is followed by the normalization of $v_i^{\mathcal{B}(R)}$ and $v_i^{\mathcal{I}(R)}$ to $\upsilon_i^{\mathcal{B}(R)}$ and $\upsilon_i^{\mathcal{I}(R)}$, respectively, for $i = 1, 2, 3$ as given in (14). Thus, Assumption 1 holds. For the S-DIR with prescribed performance, R_y is obtained by SVD [2], or for simplicity visit the Appendix in [3] with $\tilde{R} = \hat{R}R_y^\top$. The total simulation time is 30 s.

Initial attitude error is set to be considerably large. Initial attitude estimate is given by $\hat{R}(0) = \mathcal{R}_\alpha(\alpha, u/||u||)$ according to angle-axis parameterization as in (5) with $\alpha = 175$(deg) and $u = [3, 10, 8]^\top$. It is worth noting that the value of $||\tilde{R}||_I \approx 0.999$ is fairly close to the unstable equilibria $(+1)$ and the initial position is $\hat{P}(0) = [4, -3, 5]^\top$. In brief, we have

$$\boldsymbol{T}(0) = \mathbf{I}_4, \hat{\boldsymbol{T}}(0) = \begin{bmatrix} -0.8923 & 0.2932 & 0.3432 & 4 \\ 0.3992 & 0.1577 & 0.9032 & -3 \\ 0.2107 & 0.9430 & -0.2577 & 5 \\ 0 & 0 & 0 & 1 \end{bmatrix}.$$

The design parameters of the proposed filters are chosen as $\gamma = 1$, $k_w = 5$, $\bar{\delta} = \underline{\delta} = [1.3, 5, 4, 6]^\top$, $\xi^0 = [1.3, 5, -4, 6]^\top$, $\xi^\infty = [0.07, 0.3, 0.3, 0.3]^\top$, and $\ell = [4, 4, 4, 4]^\top$. The initial bias estimates are $\hat{b}_\Omega(0) = [0, 0, 0]^\top$ and $\hat{b}_V(0) = [0, 0, 0]^\top$.

Color notation used in the plots is: black center-lines and green solid-lines refer to the true values, red illustrates the performance of the nonlinear S-DIR on $\mathbb{SE}(3)$ proposed in Section IV-A, and blue demonstrates the performance of the DIR on $\mathbb{SE}(3)$ presented in Section IV-B. Also, magenta depicts a measured value while orange and black dashed lines refer to the prescribed performance response.

Figs. 3–5 depict the high values of noise and bias components attached to velocity and body-frame vector measurements plotted against the true values. Figs. 6 and 7 show the output performance of the proposed filters described in terms of Euler angles (ϕ, θ, ψ) and the true position in 3-D space,

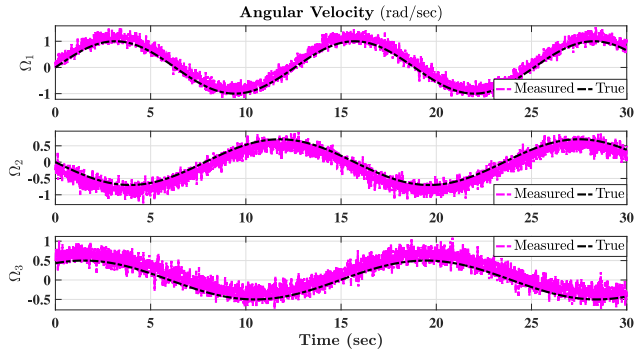

Fig. 3. Measured and true values of angular velocities.

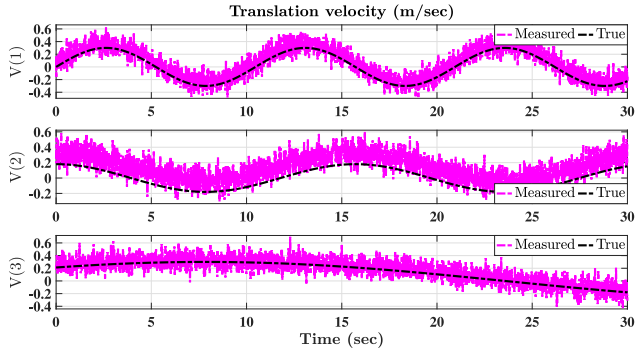

Fig. 4. Measured and true values of translational velocities.

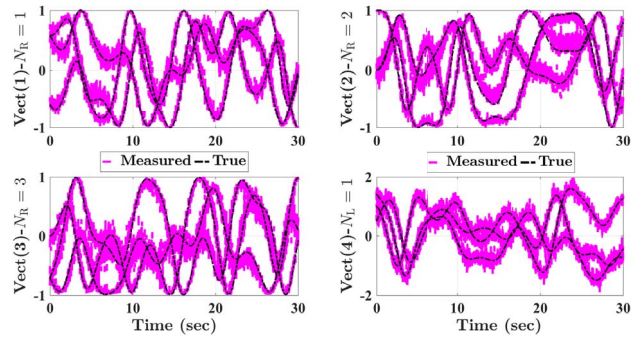

Fig. 5. True and measured body-frame vectorial measurements.

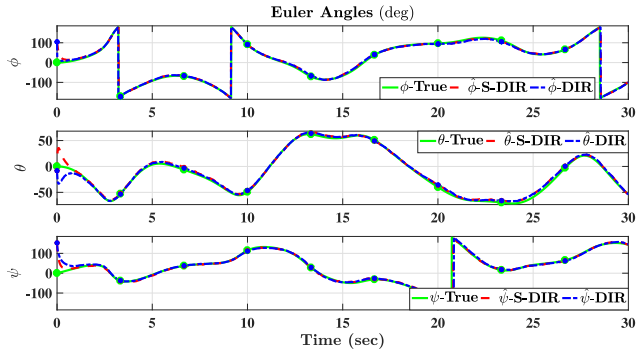

Fig. 6. True and estimated Euler angles of the rigid-body.

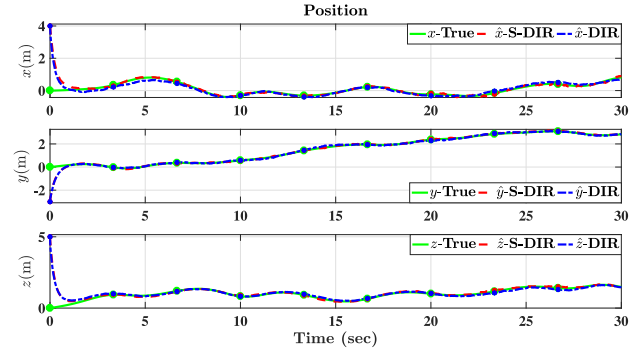

Fig. 7. True and estimated rigid-body positions in 3-D space.

respectively. Figs. 6 and 7 present the remarkable tracking performance with fast convergence to the true Euler angles and *xyz*-positions 3-D space. The systematic and smooth convergence of the error vector $\boldsymbol{e}$ is depicted in Fig. 8. It can be clearly observed how $||\tilde{R}||_I$ in Fig. 8 started very near to the unstable equilibria while $\tilde{P}_1$, $\tilde{P}_2$, and $\tilde{P}_3$ started remarkably far from the origin within the predefined large set and decayed smoothly and systematically to the predefined small set guided by the dynamic boundaries of the PPF such that $\tilde{R} = \hat{R}R^\top$ and $\tilde{P} = \hat{P} - \tilde{R}P$. Finally, the estimated bias $\hat{b}$ is bounded as depicted in Fig. 9.

The simulation results establish the strong filtering capability of the two proposed pose filters and their robustness against uncertain measurements and large initialized errors making them perfectly fit for the measurements obtained from low-quality sensors, such as IMU. The two filters confirm to the dynamic constraints imposed by the user referring guaranteed prescribed performance measures in transient as well as steady-state performance. The pose filters previously proposed in [11]–[16] lack this remarkable quality. S-DIR with prescribed performance demands pose reconstruction; in this case, attitude has been extracted using SVD [2]. This adds complexity and, therefore, the S-DIR requires more computational power in comparison with the direct pose filter with prescribed performance. Nevertheless, the two proposed pose filters are robust and demonstrate impressive convergence capabilities.

VI. Conclusion

Two nonlinear pose filters evolved directly on $\mathbb{SE}(3)$ with prescribed performance characteristics have been considered. Pose error has been defined in terms of position error and normalized Euclidean distance error, and the innovation term has been selected to guarantee predefined measures of transient and steady-state performance. As a result, the proposed filters exhibit superior convergence properties with transient error being bounded by a predefined dynamically decreasing constrained function and steady-state error being less than a predefined lower bound. The proposed pose filters are deterministic and the stability analysis ensures the boundedness of all the closed-loop signals with asymptotic convergence of the homogeneous transformation matrix to the origin. Simulation results established the strong ability of the proposed filters to impose the predefined constraints on the pose error considering large initial pose error and high level of uncertainties in the measurements.

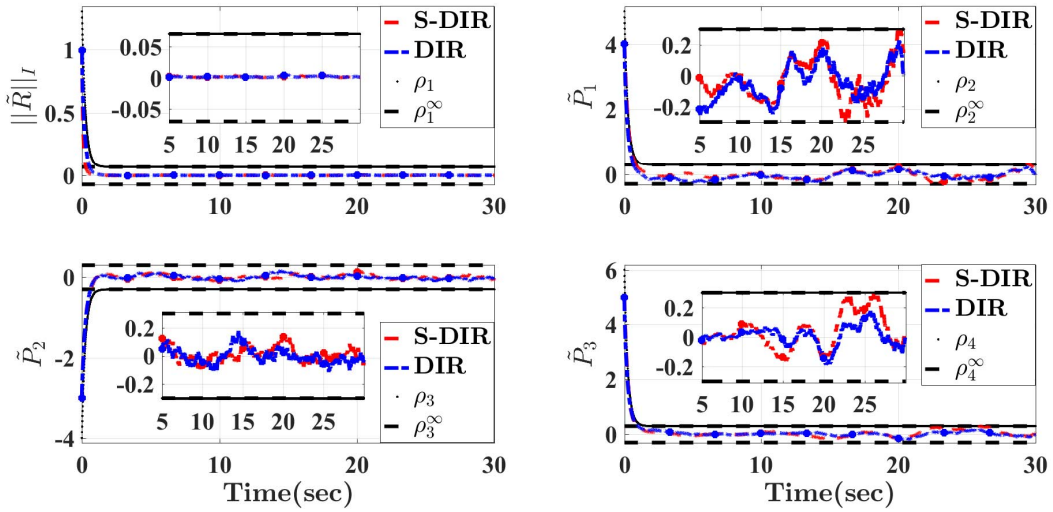

Fig. 8. Systematic convergence of the error trajectories within the prescribed performance boundaries.

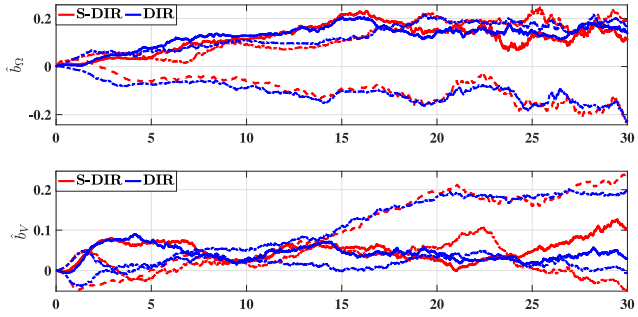

Fig. 9. Estimated bias of the proposed filters.

APPENDIX
PROOF OF LEMMA 1

Let $R \in \mathbb{SO}(3)$ be the attitude of a rigid-body in 3-D space. The attitude could be extracted for a given Rodriguez parameters vector $\rho \in \mathbb{R}^3$. The mapping from the Rodriguez vector to $\mathbb{SO}(3)$ is defined by $\mathcal{R}_\rho : \mathbb{R}^3 \to \mathbb{SO}(3)$ [31]

$$\mathcal{R}_\rho(\rho) = \frac{1}{1+||\rho||^2}\Big(\Big(1-||\rho||^2\Big)\mathbf{I}_3 + 2\rho\rho^\top + 2[\rho]_\times\Big). \tag{87}$$

With direct substitution of (87) in (4) one easily obtains [3]

$$||R||_I = \frac{||\rho||^2}{1+||\rho||^2}. \tag{88}$$

Additionally, for $\mathcal{R}_\rho = \mathcal{R}_\rho(\rho)$, the anti-symmetric projection operator of the attitude in (87) is equivalent to

$$\mathcal{P}_a(R) = \frac{1}{2}\Big(\mathcal{R}_\rho - \mathcal{R}_\rho^\top\Big) = 2\frac{1}{1+||\rho||^2}[\rho]_\times. \tag{89}$$

Thus, the vex operator of (89) becomes

$$\mathbf{vex}(\mathcal{P}_a(R)) = 2\frac{\rho}{1+||\rho||^2}. \tag{90}$$

From the result in (88), one can obtain

$$(1-||R||_I)||R||_I = \frac{||\rho||^2}{\big(1+||\rho||^2\big)^2} \tag{91}$$

and from (90), it is easily shown that

$$||\mathbf{vex}(\mathcal{P}_a(R))||^2 = 4\frac{||\rho||^2}{\big(1+||\rho||^2\big)^2}. \tag{92}$$

Therefore, (91) and (92) prove (28) in Lemma 1. From Section IV-B, $\sum_{i=1}^{N_R} k_i^R = 3$, which indicates that $\mathrm{Tr}\{\mathbf{M}_R\} = 3$. Recall that the normalized Euclidean distance of $R\mathbf{M}_R$ is $\|R\mathbf{M}_R\|_I = (1/4)\mathrm{Tr}\{(\mathbf{I}_3 - R)\mathbf{M}_R\}$. From the angle-axis parameterization in (5), one finds

$$\begin{aligned}\|R\mathbf{M}_R\|_I &= \frac{1}{4}\mathrm{Tr}\Big\{-\Big(\sin(\theta)[u]_\times + (1-\cos(\theta))[u]_\times^2\Big)\mathbf{M}_R\Big\}\\ &= -\frac{1}{4}\mathrm{Tr}\Big\{(1-\cos(\theta))[u]_\times^2\mathbf{M}_R\Big\}\end{aligned} \tag{93}$$

where $\mathrm{Tr}\{[u]_\times\mathbf{M}_R\} = 0$ as in identity (10). One has [32]

$$\|R\|_I = \frac{1}{4}\mathrm{Tr}\{\mathbf{I}_3 - R\} = \sin^2(\theta/2). \tag{94}$$

The Rodriguez vector can be expressed in terms of angle-axis parameterization as [31]

$$u = \cot(\theta/2)\rho. \tag{95}$$

From identity (8) and (95), the expression in (93) becomes

$$\|R\mathbf{M}_R\|_I = \frac{1}{2}\|R\|_I u^\top\bar{\mathbf{M}}_R u = \frac{1}{2}\|R\|_I\cot^2\Big(\frac{\theta}{2}\Big)\rho^\top\bar{\mathbf{M}}_R\rho.$$

Also, from (94), $\cos^2(\theta/2) = 1 - \|R\|_I$ which implies that

$$\tan^2\Big(\frac{\theta}{2}\Big) = \frac{\|R\|_I}{1-\|R\|_I}.$$

Accordingly, the normalized Euclidean distance of $R\mathbf{M}_R$ could be formulated in the sense of Rodriguez vector

$$\|R\mathbf{M}_R\|_I = \frac{1}{2}(1-\|R\|_I)\rho^\top\bar{\mathbf{M}}_R\rho = \frac{1}{2}\frac{\rho^\top\bar{\mathbf{M}}_R\rho}{1+\|\rho\|^2}. \tag{96}$$

The anti-symmetric projection operator of $R\mathbf{M}_R$ can be defined in terms of the Rodriguez vector using identity (6) and (9) by

$$\begin{aligned}\mathcal{P}_a(R\mathbf{M}_R) &= \frac{\rho\rho^\top\mathbf{M}_R - \mathbf{M}_R\rho\rho^\top + \mathbf{M}_R[\rho]_\times + [\rho]_\times\mathbf{M}_R}{1+\|\rho\|^2} \\ &= \frac{\left[\left(\mathrm{Tr}\{\mathbf{M}_R\}\mathbf{I}_3 - \mathbf{M}_R - [\rho]_\times\mathbf{M}_R\right)\rho\right]_\times}{1+\|\rho\|^2}.\end{aligned}$$

Thereby, the vex operator of the above expression is

$$\mathbf{vex}(\mathcal{P}_a(R\mathbf{M}_R)) = \frac{\left(\mathbf{I}_3 + [\rho]_\times\right)}{1+\|\rho\|^2}\bar{\mathbf{M}}_R\rho. \tag{97}$$

Hence, the 2-norm of (97) is equivalent to

$$\|\mathbf{vex}(\mathcal{P}_a(R\mathbf{M}_R))\|^2 = \frac{\rho^\top\bar{\mathbf{M}}_R\left(\mathbf{I}_3 - [\rho]_\times^2\right)\bar{\mathbf{M}}_R\rho}{\left(1+\|\rho\|^2\right)^2}.$$

From the identity in (8), $[\rho]_\times^2 = -||\rho||^2\mathbf{I}_3 + \rho\rho^\top$ such that

$$\begin{aligned}\|\mathbf{vex}(\mathcal{P}_a(R\mathbf{M}_R))\|^2 &= \frac{\rho^\top\bar{\mathbf{M}}_R\left(\mathbf{I}_3 - [\rho]_\times^2\right)\bar{\mathbf{M}}_R\rho}{\left(1+\|\rho\|^2\right)^2} \\ &= \frac{\rho^\top\left(\bar{\mathbf{M}}_R\right)^2\rho}{1+\|\rho\|^2} - \frac{\left(\rho^\top\bar{\mathbf{M}}_R\rho\right)^2}{\left(1+\|\rho\|^2\right)^2} \\ &\geq \underline{\lambda}\left(1 - \frac{\|\rho\|^2}{1+\|\rho\|^2}\right)\frac{\rho^\top\bar{\mathbf{M}}_R\rho}{1+||\rho||^2} \\ &\geq 2\underline{\lambda}(1-\|R\|_I)\|R\mathbf{M}_R\|_I \end{aligned} \tag{98}$$

where $\underline{\lambda} = \underline{\lambda}(\bar{\mathbf{M}}_R)$ is the minimum singular value of $\bar{\mathbf{M}}_R$ and $\|R\|_I = \|\rho\|^2/(1+\|\rho\|^2)$ as in (88). One can find

$$1 - \|R\|_I = \frac{1}{4}\left(1 + \mathrm{Tr}\left\{R\mathbf{M}_R\mathbf{M}_R^{-1}\right\}\right). \tag{99}$$

Hence, from (98) and (99) the following inequality holds:

$$\|\mathbf{vex}(\mathcal{P}_a(R\mathbf{M}_R))\|^2 \;\geq \frac{\underline{\lambda}}{2}\left(1 + \mathrm{Tr}\left\{R\mathbf{M}_R\mathbf{M}_R^{-1}\right\}\right)\|R\mathbf{M}_R\|_I.$$

This validates (29) and completes the proof of Lemma 1.

ACKNOWLEDGMENT

The authors would like to thank Maria Shaposhnikova for proofreading this paper.

REFERENCES

[1] M. D. Shuster and S. D. Oh, "Three-axis attitude determination from vector observations," *J. Guid. Control Dyn.*, vol. 4, no. 1, pp. 70–77, 1981.

[2] F. L. Markley, "Attitude determination using vector observations and the singular value decomposition," *J. Astronautical Sci.*, vol. 36, no. 3, pp. 245–258, 1988.

[3] H. A. Hashim, L. J. Brown, and K. McIsaac, "Nonlinear stochastic attitude filters on the special orthogonal group 3: ITO and stratonovich," *IEEE Trans. Syst., Man, Cybern., Syst.*, to be published.

[4] D. Choukroun, I. Y. Bar-Itzhack, and Y. Oshman, "Novel quaternion Kalman filter," *IEEE Trans. Aerosp. Electron. Syst.*, vol. 42, no. 1, pp. 174–190, Jan. 2006.

[5] E. J. Lefferts, F. L. Markley, and M. D. Shuster, "Kalman filtering for spacecraft attitude estimation," *J. Guid. Control Dyn.*, vol. 5, no. 5, pp. 417–429, 1982.

[6] F. L. Markley, "Attitude error representations for Kalman filtering," *J. Guid. Control Dyn.*, vol. 26, no. 2, pp. 311–317, 2003.

[7] R. Mahony, T. Hamel, and J.-M. Pflimlin, "Nonlinear complementary filters on the special orthogonal group," *IEEE Trans. Autom. Control*, vol. 53, no. 5, pp. 1203–1218, Jun. 2008.

[8] H. A. Hashim, L. J. Brown, and K. McIsaac, "Nonlinear explicit stochastic attitude filter on SO(3)," in *Proc. 57th IEEE Conf. Decis. Control (CDC)*, 2018, pp. 1210–1216.

[9] H. F. Grip, T. I. Fossen, T. A. Johansen, and A. Saberi, "Attitude estimation using biased gyro and vector measurements with time-varying reference vectors," *IEEE Trans. Autom. Control*, vol. 57, no. 5, pp. 1332–1338, May 2012.

[10] S. Q. Liu and R. Zhu, "A complementary filter based on multi-sample rotation vector for attitude estimation," *IEEE Sensors J.*, vol. 18, no. 16, pp. 6686–6692, Aug. 2018.

[11] H. Rehbinder and B. K. Ghosh, "Pose estimation using line-based dynamic vision and inertial sensors," *IEEE Trans. Autom. Control*, vol. 48, no. 2, pp. 186–199, Feb. 2003.

[12] G. Baldwin, R. Mahony, J. Trumpf, T. Hamel, and T. Cheviron, "Complementary filter design on the special Euclidean group SE(3)," in *Proc. Eur. Control Conf. (ECC)*, 2007, pp. 3763–3770.

[13] H. A. Hashim, L. J. Brown, and K. McIsaac, "Nonlinear stochastic position and attitude filter on the special Euclidean group 3," *J. Frankl. Inst.*, vol. 356, no. 7, pp. 4144–4173, 2019.

[14] G. Baldwin, R. Mahony, and J. Trumpf, "A nonlinear observer for 6 DOF pose estimation from inertial and bearing measurements," in *Proc. IEEE Int. Conf. Robot. Autom. (ICRA)*, 2009, pp. 2237–2242.

[15] M.-D. Hua, T. Hamel, R. Mahony, and J. Trumpf, "Gradient-like observer design on the special Euclidean group SE(3) with system outputs on the real projective space," in *Proc. IEEE 54th Annu. Conf. Decis. Control (CDC)*, 2015, pp. 2139–2145.

[16] J. F. Vasconcelos, R. Cunha, C. Silvestre, and P. Oliveira, "A nonlinear position and attitude observer on SE(3) using landmark measurements," *Syst. Control Lett.*, vol. 59, nos. 3–4, pp. 155–166, 2010.

[17] S. Dominguez, "Simultaneous recognition and relative pose estimation of 3D objects using 4D orthonormal moments," *Sensors (Basel)*, vol. 17, no. 9, p. 2122, 2017.

[18] M.-D. Hua and G. Allibert, "Riccati observer design for pose, linear velocity and gravity direction estimation using landmark position and IMU measurements," in *Proc. IEEE Conf. Control Technol. Appl.*, 2018, pp. 1313–1318.

[19] M. Tanaka, K. Tanaka, and H. O. Wang, "Practical model construction and stable control of an unmanned aerial vehicle with a parafoil-type wing," *IEEE Trans. Syst., Man, Cybern., Syst*, vol. 49, no. 6, pp. 1291–1297, Jun. 2019.

[20] F. Santoso, M. A. Garratt, S. G. Anavatti, and I. Petersen, "Robust hybrid nonlinear control systems for the dynamics of a quadcopter drone," *IEEE Trans. Syst., Man, Cybern., Syst*, to be published.

[21] L. Sun, W. Huo, and Z. Jiao, "Disturbance observer-based robust relative pose control for spacecraft rendezvous and proximity operations under input saturation," *IEEE Trans. Aerosp. Electron. Syst.*, vol. 54, no. 4, pp. 1605–1617, Aug. 2018.

[22] T. Lee, "Geometric control of quadrotor UAVs transporting a cable-suspended rigid body," *IEEE Trans. Control Syst. Technol.*, vol. 26, no. 1, pp. 255–264, Jan. 2018.

[23] C. P. Bechlioulis and G. A. Rovithakis, "Robust adaptive control of feedback linearizable MIMO nonlinear systems with prescribed performance," *IEEE Trans. Autom. Control*, vol. 53, no. 9, pp. 2090–2099, Oct. 2008.

[24] M. Wang and A. Yang, "Dynamic learning from adaptive neural control of robot manipulators with prescribed performance," *IEEE Trans. Syst., Man, Cybern., Syst*, vol. 47, no. 8, pp. 2244–2255, Aug. 2017.

[25] Y. Yang, J. Tan, and D. Yue, "Prescribed performance tracking control of a class of uncertain pure-feedback nonlinear systems with input saturation," *IEEE Trans. Syst., Man, Cybern., Syst*, to be published.

[26] J. Na, Q. Chen, X. Ren, and Y. Guo, "Adaptive prescribed performance motion control of servo mechanisms with friction compensation," *IEEE Trans. Ind. Electron.*, vol. 61, no. 1, pp. 486–494, Jan. 2014.

[27] H. A. Hashim, S. El-Ferik, and F. L. Lewis, "Neuro-adaptive cooperative tracking control with prescribed performance of unknown higher-order nonlinear multi-agent systems," *Int. J. Control*, vol. 92, no. 2, pp. 445–460, 2019.

[28] H. A. Hashim, S. El-Ferik, and F. L. Lewis, "Adaptive synchronisation of unknown nonlinear networked systems with prescribed performance," *Int. J. Syst. Sci.*, vol. 48, no. 4, pp. 885–898, 2017.

[29] H. A. Hashim, L. J. Brown, and K. McIsaac, "Guaranteed performance of nonlinear attitude filters on the special orthogonal group SO(3)," *IEEE Access*, vol. 7, pp. 3731–3745, 2019.

[30] F. Bullo and A. D. Lewis, *Geometric Control of Mechanical Systems: Modeling, Analysis, and Design for Simple Mechanical Control Systems*, vol. 49. New York, NY, USA: Springer, 2004.
[31] M. D. Shuster, "A survey of attitude representations," *Navigation*, vol. 8, no. 9, pp. 439–517, 1993.
[32] R. M. Murray, Z. Li, and S. S. Sastry, *A Mathematical Introduction to Robotic Manipulation*. Boca Raton, FL, USA: CRC Press, 1994.

Hashim A. Hashim (S'18) received the bachelor's degree in mechatronics from the Department of Mechanical Engineering, Helwan University, Helwan, Egypt, and the M.Sc. degree in systems and control engineering from the Department of Systems Engineering, King Fahd University of Petroleum and Minerals, Dhahran, Saudi Arabia. He is currently pursuing the Ph.D. degree in robotics and control with the Department of Electrical and Computer Engineering, Western University, London, ON, Canada.

His current research interests include stochastic and deterministic attitude and pose filters, control of multiagent systems, control applications, and optimization techniques.

Lyndon J. Brown received the B.Sc. degree in electrical engineering from the University of Waterloo, Waterloo, ON, Canada, in 1988 and the M.Sc. and Ph.D. degrees in electrical engineering from the University of Illinois at Urbana–Champaign, Champaign, IL, USA, in 1991 and 1996, respectively.

He is an Associate Professor with the Department of Electrical and Computer Engineering, Western University, London, ON, Canada. He was with Honeywell Aerospace Canada, Mississauga, ON, Canada, and E.I. DuPont de Nemours, Midland, MI, USA. His current research interests include identification and control of predictable signals, biological control systems, welding control systems, and attitude and pose estimation.

Kenneth McIsaac (M'99) received the B.Sc. degree in electrical engineering from the University of Waterloo, Waterloo, ON, Canada, in 1996 and the M.Sc. and Ph.D. degrees in electrical engineering from the University of Pennsylvania, Philadelphia, PA, USA, in 1998 and 2001, respectively.

He is currently an Associate Professor and the Chair of Electrical and Computer Engineering with Western University, London, ON, Canada. His current research interests include computer vision and signal processing, mostly in the context of using machine intelligence in robotics and assistive systems, and attitude and pose estimation.